

Arterial Spin Labeling (ASL) in Neuroradiological Diagnostics – Methodological Overview and Use Cases

Arterial Spin Labeling (ASL) in der neuroradiologischen Diagnostik – Methodischer Überblick und Anwendungsfälle

Authors

Nico Sollmann^{1, 2, 3, 4}, Gabriel Hoffmann^{2, 3}, Severin Schramm², Miriam Reichert², Moritz Hernandez Petzsche², Joachim Strobel⁵, Lorenzo Nigris⁴, Christopher Kloth¹, Johannes Rosskopf^{1, 6}, Corinna Börner^{2, 7, 8}, Michaela Bonfert^{7, 8}, Maria Berndt², Georg Grön⁹, Hans-Peter Müller¹⁰, Jan Kassubek^{10, 11}, Kornelia Kreiser^{1, 12}, Inga K. Koerte^{4, 13, 14}, Hans Liebl^{2, 15}, Ambros Beer^{5, 16, 17}, Claus Zimmer^{2, 3}, Meinrad Beer^{1, 16, 17}, Stephan Kaczmarz^{2, 3, 18}

Affiliations

- 1 Department of Diagnostic and Interventional Radiology, University Hospital Ulm, Ulm, Germany
- 2 Department of Diagnostic and Interventional Neuroradiology, School of Medicine, Klinikum rechts der Isar, Technical University of Munich, Munich, Germany
- 3 TUM-Neuroimaging Center, Klinikum rechts der Isar, Technical University of Munich, Munich, Germany
- 4 cBrain, Department of Child and Adolescent Psychiatry, Psychosomatics, and Psychotherapy, Ludwig-Maximilians-Universität München, Munich, Germany
- 5 Department of Nuclear Medicine, University Hospital Ulm, Ulm, Germany
- 6 Section of Neuroradiology, Bezirkskrankenhaus Günzburg, Günzburg, Germany
- 7 LMU Hospital, Department of Pediatrics – Dr. von Hauner Children's Hospital, Division of Pediatric Neurology and Developmental Medicine, Ludwig-Maximilians-Universität München, Munich, Germany
- 8 LMU Center for Children with Medical Complexity – iSPZ Hauner, Ludwig-Maximilians-Universität München, Munich, Germany
- 9 Department of Psychiatry and Psychotherapy III, University Hospital Ulm, Ulm, Germany
- 10 Department of Neurology, University Hospital Ulm, Ulm, Germany
- 11 German Center for Neurodegenerative Diseases (DZNE), Ulm University, Ulm, Germany
- 12 Department of Radiology and Neuroradiology, Universitäts- und Rehabilitationskliniken Ulm, Ulm, Germany
- 13 Psychiatry Neuroimaging Laboratory, Department of Psychiatry, Brigham and Women's Hospital, Boston, United States
- 14 Department of Psychiatry, Harvard Medical School, Massachusetts General Hospital, Boston, United States
- 15 Department of Radiology, Berufsgenossenschaftliche Unfallklinik Murnau, Murnau, Germany
- 16 MoMan – Center for Translational Imaging, University Hospital Ulm, Ulm, Germany

17 i2Soul – Innovative Imaging in Surgical Oncology, University Hospital Ulm, Ulm, Germany
18 Market DACH, Philips GmbH, Hamburg, Germany

Key words

arterial spin labeling, perfusion, cerebral blood flow, cerebrovascular disease, ischemia

received 07.02.2023

accepted 12.06.2023

published online 19.07.2023

Bibliography

Fortschr Röntgenstr 2024; 196: 36–51

DOI 10.1055/a-2119-5574

ISSN 1438-9029

© 2023. Thieme. All rights reserved.

Georg Thieme Verlag KG, Rüdigerstraße 14, 70469 Stuttgart, Germany

Correspondence

Dr. Nico Sollmann

Department of Diagnostic and Interventional Radiology, University Hospital Ulm, Albert-Einstein-Allee 23, 89081 Ulm, Germany

Tel.: +49/7 31/50 06 10 01

nico.sollmann@tum.de

ABSTRACT

Background Arterial spin labeling (ASL) is a magnetic resonance imaging (MRI)-based technique using labeled blood-water of the brain-feeding arteries as an endogenous tracer to derive information about brain perfusion. It enables the assessment of cerebral blood flow (CBF).

Method This review aims to provide a methodological and technical overview of ASL techniques, and to give examples of clinical use cases for various diseases affecting the central nervous system (CNS). There is a special focus on recent developments including super-selective ASL (ssASL) and time-resolved ASL-based magnetic resonance angiography (MRA)

and on diseases commonly not leading to characteristic alterations on conventional structural MRI (e. g., concussion or migraine).

Results ASL-derived CBF may represent a clinically relevant parameter in various pathologies such as cerebrovascular diseases, neoplasms, or neurodegenerative diseases. Furthermore, ASL has also been used to investigate CBF in mild traumatic brain injury or migraine, potentially leading to the establishment of imaging-based biomarkers. Recent advances made possible the acquisition of ssASL by selective labeling of single brain-feeding arteries, enabling spatial perfusion territory mapping dependent on blood flow of a specific preselected artery. Furthermore, ASL-based MRA has been introduced, providing time-resolved delineation of single intracranial vessels.

Conclusion Perfusion imaging by ASL has shown promise in various diseases of the CNS. Given that ASL does not require intravenous administration of a gadolinium-based contrast agent, it may be of particular interest for investigations in pediatric cohorts, patients with impaired kidney function, patients with relevant allergies, or patients that undergo serial MRI for clinical indications such as disease monitoring.

Key Points:

- ASL is an MRI technique that uses labeled blood-water as an endogenous tracer for brain perfusion imaging.
- It allows the assessment of CBF without the need for administration of a gadolinium-based contrast agent.
- CBF quantification by ASL has been used in several pathologies including brain tumors or neurodegenerative diseases.
- Vessel-selective ASL methods can provide brain perfusion territory mapping in cerebrovascular diseases.
- ASL may be of particular interest in patient cohorts with caveats concerning gadolinium administration.

ZUSAMMENFASSUNG

Hintergrund Arterial spin labeling (ASL) ist eine Technik der Magnetresonanztomographie (MRT), die eine Markierung des einströmenden Bluts der hirnersorgenden Arterien als endogenen Tracer verwendet, um Informationen über die Hirnperfusion zu generieren. Die Technik ermöglicht eine Untersuchung des zerebralen Blutflusses (CBF).

Methode Diese Übersichtsarbeit möchte einen methodischen und technischen Überblick über die ASL-Techniken vermitteln und Beispiele für klinische Anwendungsfälle anhand von verschiedenen Erkrankungen des zentralen Nervensystems (ZNS) vorstellen. Ein besonderer Fokus liegt dabei auf jüngsten Entwicklungen im Bereich der super-selektiven ASL

(ssASL) und zeitaufgelösten ASL-basierten Magnetresonanz-Angiographie (MRA) sowie auf Erkrankungen, die üblicherweise nicht zu charakteristischen Veränderungen gemäß konventioneller struktureller MRT führen (beispielsweise Gehirnerschütterungen oder Migräne).

Ergebnisse Der aus ASL generierte CBF kann einen klinisch relevanten Parameter in Zusammenhang mit verschiedenen Pathologien des ZNS darstellen, wie zum Beispiel bei zerebrovaskulären Erkrankungen, Neoplasien oder neurodegenerativen Erkrankungen. Des Weiteren wurde ASL zur Untersuchung des CBF bei mildem Schädel-Hirn-Trauma oder auch bei Migräne angewendet, so dass potenziell bildbasierte Biomarker etabliert werden könnten. Neuere Entwicklungen ermöglichen zudem die Akquisition von ssASL über eine selektive Markierung einzelner hirnersorgender Arterien, was eine räumlich aufgelöste Kartierung von Perfusionsterritorien basierend auf dem Blutfluss eines spezifischen vorausgewählten Gefäßes zulässt. Daneben wurde auch eine ASL-basierte MRA umgesetzt, die eine zeitaufgelöste Darstellung einzelner intrakranieller Gefäßäste möglich macht.

Schlussfolgerung Perfusionsbildgebung mittels ASL kann insbesondere vielversprechend sein bei Untersuchungen in pädiatrischen Kohorten, bei Patienten mit eingeschränkter Nierenfunktion, Patienten mit relevanten Allergien oder Patienten mit wiederholten MRT-Bildgebungen aufgrund klinischer Indikationen wie beispielsweise zum Krankheitsmonitoring, da die Technik gänzlich ohne Gabe eines Gadolinium-haltigen Kontrastmittels auskommt.

Kernaussagen:

- ASL ist eine Technik der MRT, welche die Markierung von einströmendem Blut als endogenem Tracer zur Perfusionsbildgebung verwendet.
- ASL ermöglicht die Untersuchung des CBF ohne die Gabe von Gadolinium-haltigem Kontrastmittel.
- Quantifizierungen des CBF mittels ASL wurden im Rahmen verschiedener Pathologien einschließlich Hirntumore und neurodegenerative Erkrankungen untersucht.
- Gefäß-selektive ASL-Methoden ermöglichen Kartierungen der Hirnperfusion bei zerebrovaskulären Erkrankungen.
- ASL kann insbesondere bei Patienten mit Kontraindikationen für die Gabe von Gadolinium von großer Bedeutung sein.

Zitierweise

- Sollmann N, Hoffmann G, Schramm S et al. Arterial Spin Labeling (ASL) in Neuroradiological Diagnostics – Methodological Overview and Use Cases. Fortschr Röntgenstr 2024; 196: 36–51

Introduction

Contemporary neuroimaging by magnetic resonance imaging (MRI) is comprised of multi-parametric acquisition protocols using multiple sequences that allow the radiologist to derive information about macro- and micro-structure, function, metabolism,

and/or perfusion. Such multi-parametric approaches can facilitate initial differential diagnosis, as well as disease and therapy monitoring of various pathologies affecting the central nervous system (CNS). Specifically, perfusion imaging can be achieved using several brain MRI techniques [1–3]. Most commonly in the clinical routine, information about perfusion is derived from methods

that require the intravenous application of a gadolinium-based contrast agent. Those include dynamic contrast-enhanced MRI (DCE-MRI), making use of T1 shortening effects of gadolinium during repeated acquisitions of T1-weighted images, and dynamic susceptibility contrast MRI (DSC-MRI), relating to local magnetic field distortion effects around vessels with T2* dephasing and signal loss while a bolus of gadolinium passes, captured by a series of rapidly acquired spin or gradient echo images [1, 4]. In contrast to these approaches, arterial spin labeling (ASL) works fundamentally differently since it does not require the injection of a gadolinium-based contrast agent, but instead uses blood-water as an endogenous tracer, enabling the assessment of cerebral blood flow (CBF) [5–9].

Since the introduction of the ASL method in the early 1990s, it has shown promise as a potential alternative to conventional perfusion imaging methods such as DCE- or DSC-MRI [5, 10]. With the publication of a consensus on the clinical implementation of ASL by the Perfusion Study Group of the International Society of Magnetic Resonance in Medicine (ISMRM) and the European Consortium for ASL in Dementia in 2015, the technique has been further conceptualized and the transition to broader clinical application has been facilitated [5]. This early consensus statement has been recently followed up by an overview of the current state and guidance on ASL in clinical neuroimaging with a methodological focus, published on behalf of the ISMRM Perfusion Study Group [11]. Nowadays, ASL can be part of imaging protocols for several diseases affecting the CNS, ranging from cerebrovascular diseases as the most prominent clinical application and neoplasms to concussion or migraine, which are conditions that may not even necessarily show morphological alterations on conventional structural MRI. Furthermore, the capabilities of ASL have been considerably expanded in recent years: while initial applications predominantly enabled the investigation of whole-brain perfusion, recent advances have made available vessel-selective imaging of single perfusion territories of the brain, as well as time-resolved angiography based on such vessel-selective imaging.

Against this background, this narrative review article aims to provide an overview of general methodological and technical characteristics of ASL, followed by a review of ASL applications for various diseases affecting the CNS. In this context, previous publications have provided detailed recommendations, particularly regarding the basic methodological applications of the most common ASL techniques based on major clinical use cases, while some specific ASL-based methods that are not yet widely applied (e. g., vessel-selective imaging or ASL-based angiography) or diseases that currently do not regularly require perfusion imaging (e. g., migraine or brain injury) have not been covered [5, 11]. Therefore, a special focus of the present article was to 1) provide methodological aspects and clinical examples for vessel-selective ASL and time-resolved ASL-based angiography (i. e., two advanced methods providing insights that cannot be derived from other pulse sequences such as DSC-MRI), and 2) present clinical examples for diseases that do not regularly show clear morphological

alterations on conventional MRI (i. e., ASL could deliver biomarkers for diseases such as migraine or concussion that are mostly neglected by standard neuroradiological diagnostics).

Methods and technical aspects

General overview

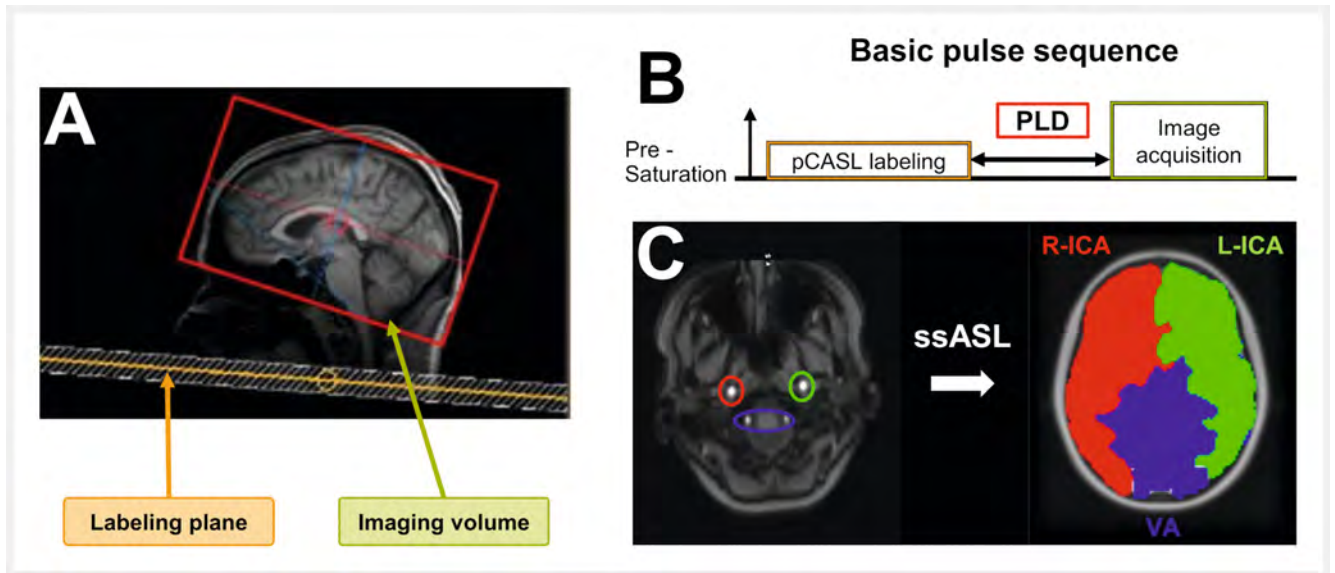
The high potential of ASL is the result of its methodological elegance. It is a noninvasive MRI technique that uses the blood-water as an endogenous tracer (► Fig. 1). As water can be assumed to be freely diffusible, ASL is particularly well suited for measuring brain perfusion. The method is based on the subtraction of label and control images, where the magnetization of blood-water is magnetically inverted during the labeling process, while no effective labeling is performed prior to the acquisition of the control image. In general, the ASL method makes it possible to quantify CBF (in ml/100 g/min) [5, 9, 11].

Historically, two different categories of labeling methods were proposed: continuous ASL (CASL) and pulsed ASL (PASL) [10, 12, 13]. While CASL offers a comparably good signal-to-noise ratio (SNR), it is limited by magnetization transfer-induced artifacts and the high amount of energy deposition in the subject. Additionally, the availability of continuous pulses is limited on most clinical MRI systems [14]. In contrast, short-pulsed schemes are widely available and result in way lower energy deposition. However, single pulses as implemented in PASL result in a comparably low SNR. Both CASL and PASL have shown promising initial applications. However, they have been used quite rarely for clinical imaging, which is due to their inherent limitations.

Pseudo-continuous ASL

A major advancement was a third approach called pseudo-continuous ASL (pCASL; ► Fig. 1), which was proposed by Dai et al. in 2008 as a hybrid of CASL and PASL [15, 16]. Conceptually being a CASL technique, the long labeling period is split into a series of short pulses, which has several advantages. First, short pulses are available on most clinical MRI systems, providing wide applicability and availability. Second, the technique results in lower energy deposition in the subject, allowing longer labeling periods. The labeling is hereby performed within a thin slice, which is often referred to as the labeling plane (► Fig. 1).

In pCASL, a post-label delay (PLD) is introduced between the labeling and image acquisition (► Fig. 1). This is set to account for the arterial transit time (ATT), which is the time it takes the labeled blood to travel from the labeling region to the tissue of interest, which is then captured by the imaging volume. The PLD is a critical parameter when setting up a pCASL sequence: short PLDs can result in underestimation of CBF, while the signal intensity will be reduced for long PLDs due to venous draining and the inherent T1 decay of the labeled spins [5]. Therefore, the consensus statement of the Perfusion Study Group of the ISMRM and the European Consortium for ASL in Dementia included consistent recommendations for the implementation of ASL sequences and the choice of parameters, such as different PLDs for different populations [5]. Furthermore, updated recommendations for the implementation of



► **Fig. 1** Acquisition and main concepts of arterial spin labeling (ASL). **A** For labeling purposes, the inflowing blood-water is magnetically labeled within the labeling plane. The labeling plane should be placed orthogonally on a straight segment of the brain-feeding arteries. **B** Prior to image acquisition, a post-label delay (PLD) is introduced to account for the time it takes the labeled blood to arrive at the imaging volume. **C** By labeling single brain-feeding arteries, super-selective ASL (ssASL) allows mapping of individual perfusion territories, for example those belonging to the right internal carotid artery (R-ICA; red area) or left ICA (L-ICA; green area) as well as to the vertebral arteries (VAs; blue area).

clinical perfusion imaging sequences using ASL have been recently provided by the ISMRM Perfusion Study Group [9, 11].

Time-encoded ASL

Instead of adapting the PLD to the respective study cohorts (e. g., in terms of age), multiple PLDs can be acquired, which can be used to fit a kinetic model to estimate the CBF and ATT (e. g., Buxton general kinetic model) [17]. This can greatly improve quantitative CBF estimates, as it accounts for intra- and inter-subject ATT variations. In general, multi-PLD data can be obtained by acquiring multiple single-PLD datasets with variations of the PLD between each scan. However, this results in rather long scan times, which may not be feasible for clinical imaging protocols. Therefore, several approaches have been proposed to acquire multi-PLD data [18–22].

One readout-based approach uses Look-Locker sampling, which basically employs a series of low flip angle excitations during the relaxation of the longitudinal magnetization to the thermal equilibrium, which allows image acquisition with a considerably high number of different delays [18, 19]. However, the readout pulse train will effectively reduce the amount of signal available for later PLDs, resulting in a reduced SNR [20]. As an alternative, Günther et al. proposed a time-encoded labeling scheme based on CASL, which was later also adapted for pCASL [21, 22]. By alternating label and control conditions according to a Hadamard matrix, decoded images can be acquired in a highly time-efficient manner. Those images can be decoded during post-processing, resulting in CBF and ATT maps within clinically feasible scan times.

ASL-based perfusion territory mapping

All whole-brain ASL implementations including pCASL perform non-selective labeling of the blood-water flowing through all the brain-feeding arteries. However, especially in steno-occlusive diseases, variations in blood supply between different perfusion territories are a typical scenario. Therefore, vessel-selective imaging could be of high clinical impact, allowing the noninvasive determination of individual perfusion territories. In this regard, different approaches have been proposed. Based on PASL, rotated labeling slabs have been used that have been manually placed onto the major brain-feeding arteries [23, 24]. However, this comes with the inherent drawbacks of PASL and does not provide high spatial selectivity. Another approach is vessel-encoded ASL, where off-resonance effects introduced by gradients are used to generate effective labeling regions [25, 26]. Although it is time-efficient, the method is based on population-averaged distances between the internal carotid arteries (ICAs) and the vertebral arteries (VAs) and is less sensitive for collateral blood supply.

However, specific vessel-selective labeling can be facilitated by super-selective ASL (ssASL), which was proposed by Helle et al. based on pCASL [27]. Time-varying gradients are applied perpendicular to the selected area and result in effective labeling spots. Thus, ssASL provides a high degree of freedom in placing the labeling spot together with high spatial selectivity. Clinical applicability was further enhanced by options for automated planning of the labeling spots [28]. Recently, a combination of ssASL labeling with the contrast-enhanced timing-robust angiography (CENTRA) keyhole technique and view-sharing was proposed (4D-sPACK), leading to noninvasive and time-resolved ASL angiography with clinically reasonable scan times of less than 5 minutes per labeled vessel [29, 30].

Approaches to ASL data processing and analysis

Post-processing of acquired ASL data regularly includes control-label subtraction and averaging of the subtraction series, which could be extended by additional steps for motion correction or outlier scrubbing [9, 11]. Depending on the particular clinical use case, further post-processing steps might be helpful for data interpretation, such as partial volume correction (e. g., to remove pseudo-hypoperfusion effects secondary to cerebral atrophy in neurodegenerative diseases [ND]) or normalization to normal-appearing brain parenchyma (e. g., to potentially improve accuracy for brain tumor grading) [9, 11, 31, 32]. For pCASL as today's most common ASL-based method, generation of perfusion maps and quantification of CBF can be obtained. Typically, pCASL is used to derive information on whole-brain perfusion, but segmentation (e. g., by co-registration with anatomical T1-weighted or T2-weighted sequences) can be added to derive more localized information from a lesion or a specific brain structure. In contrast, ssASL provides territorial perfusion information from a preselected brain-supplying artery, thus is more dynamic and may provide the most comprehensive information when more than a single vessel is labeled successively (e. g., to derive information about perfusion territory shifts and individual cerebrovascular architecture).

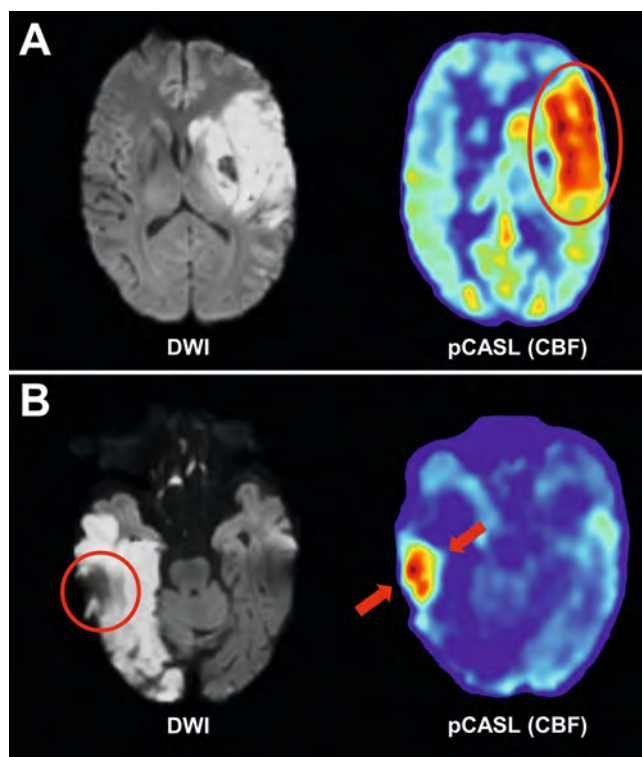
In recent years, considerable advancements have been made regarding both standardized ASL data storage as well as standardized perfusion analyses. One example is the extension of the Brain Imaging Data Structure (BIDS) for ASL data, in order to provide data storage standards that meet the need for structured image data organization, including also metadata beyond the image files (e. g., acquisition characteristics such as voxel sizes) [33, 34]. Furthermore, software packages such as ExploreASL (written in MATLAB and based on Statistical Parametric Mapping [SPM]) have been developed recently, which may facilitate standardized analysis of ASL data across centers and scanners [35]. Another software application is ASLPrep, aiming to provide a generalizable and robust workflow targeting reproducible processing of heterogeneous ASL data [36]. As such, it also provides advanced analysis approaches beyond the commonly used kinetic model for CBF quantification, including two different Bayesian models incorporating information regarding brain structure with the Bayesian Inference for ASL (BASIL) and Structural Correlation with Robust Bayesian (SCRUB) methods [36].

Clinical use cases

Cerebrovascular diseases

Ischemic stroke

Globally, stroke is ranked as the second leading cause of disability and mortality, with approximately 13.7 million incidents of stroke in 2016 [37]. Of those, more than 80% are categorized as ischemic strokes, which commonly occur on the basis of cardioembolism, large artery atherosclerosis, or vessel occlusions [37, 38]. Ischemic stroke is one of the most frequent indications for perfusion imaging by computed tomography (CT) or MRI. Perfu-



► **Fig. 2** Post-stroke perfusion imaging using pseudo-continuous arterial spin labeling (pCASL) with corresponding axial diffusion-weighted imaging (DWI), which was acquired three days after ischemic stroke due to intracranial vessel occlusions. **A** In a 55-year-old female patient, DWI showed a large infarct with diffusion restriction after thrombotic left-sided occlusion of the M1 segment, and cerebral blood flow (CBF) maps from pCASL showed marked hyperperfusion of the infarct territory that occurred after successful revascularization therapy. **B** In a 70-year-old male patient, DWI showed a large temporo-occipital infarct after right-sided thrombotic occlusion of the P1 segment, and the infarct core was markedly hypoperfused on pCASL-derived CBF maps, while a small region in the lateral aspect of the temporal lobe showed marked hyperperfusion where no diffusion restriction was observed.

sion imaging-based selection of patients for endovascular therapy and/or intravenous thrombolysis in ischemic stroke has found entrance into the clinical routine based on a large body of evidence both for CT and MRI [39–48]. In recent years, ASL has been studied many times as a potential alternative to DSC-MRI in stroke imaging (► **Fig. 2**).

Studies comparing DSC-MRI and ASL-based perfusion imaging have found overall good agreement in ischemic stroke [49, 50]. Bokkers et al. found that ASL-based perfusion may be used alternatively to DSC-MRI in penumbra imaging for acute stroke, especially in patients with contraindications to gadolinium-based contrast media [51]. Furthermore, ASL has been shown to be more sensitive than DSC-MRI for detecting post-stroke hyperperfusion, which often occurs after successful revascularization therapy [50, 52]. It should be noted that a previous study indicated that hyperperfusion may be associated with a good outcome after stroke, likely as a surrogate of successful reperfusion and reactive infarct hyperemia [52–54]. On the other hand, ASL-based hyper-

perfusion following stroke has also been suggested as a risk factor for the development of intracranial bleeding [53–55].

Post-stroke (hyper-)perfusion could become a clinically relevant imaging marker, but thus far it is unclear at what threshold the risk of intracranial bleeding overtakes potential physiological benefits. Due to its sensitivity to post-stroke hyperperfusion, ASL seems especially suitable for studying this phenomenon and may be used in the future to screen for patients that are at high risk for the development of infarct bleeding.

Arteriovenous malformations/Moyamoya disease

Pre-treatment imaging of brain arteriovenous malformations (AVMs) is usually performed with digital subtraction angiography (DSA) as the reference standard [56]. A noninvasive alternative for vessel-selective angiography is time-resolved ASL-based 4D-sPACK (► Fig. 3). Specifically, it has been shown that this method could reliably identify arterial feeders, nidus size, and venous drainage in comparison to DSA in a series of 15 AVMs [30]. Furthermore, a case report showed high visual concordance between DSA and ASL-based MRA and demonstrated the feasibility of the segmentation of vascular territories and border zones using perfusion maps [57]. Furthermore, ASL has been used to monitor treatment success after radiosurgery for AVMs by enabling confirmation of the obliteration or detection of residual manifestations following treatment [58, 59]. As a potential advantage compared to DSA, ASL-based MRA is not affected by intravascular pressure changes resulting from contrast medium application through a syringe, which may be beneficial when trying to understand the hemodynamics of an AVM.

Moyamoya disease, often characterized by progressive stenoses of the distal ICA and its proximal branches with associated characteristic micro-collateralization, is also highly accessible to ASL-based imaging including ASL-based MRA (► Fig. 4). Due to alterations of the vascular architecture during the disease course of Moyamoya, severe and rapid changes in brain hemodynamics can be observed [60, 61]. Previous studies have indicated good agreement between DSC-MRI and ASL-based perfusion imaging for the monitoring of cerebral hemodynamic changes before and after bypass surgery [60, 61].

Internal carotid artery stenosis

Usually caused by atherosclerotic plaques at the inner arterial wall, the prevalence of ICA stenosis (ICAS) $\geq 50\%$ in patients with acute ischemic stroke ranges between approximately 15% and 20% [62–64]. Besides ischemia, the persistently reduced blood supply of the brain can manifest as severe chronic perfusion deficits and may result in cognitive decline [65]. Both symptomatic patients with previous signs of permanent cerebral ischemia and transient ischemic attacks, as well as asymptomatic patients with no obvious symptoms coexist in the case of ICAS.

Current diagnostic procedures usually rely on estimations of the degree of stenosis by extracranial Doppler ultrasound [66, 67]. Even with additional CT angiography (CTA) or MRA, information on the complex local effects of ICAS on brain tissue (e. g., collateral blood flow) is limited. Furthermore, while contrast agent-based perfusion imaging methods such as DSC-MRI are promising

especially with regards to the imaging of regional perfusion delay, collateral pathways cannot be detected even though they are known to severely alter stroke risk patterns in ICAS [65, 68]. Thus, ASL has high potential as a noninvasive imaging tool to quantify regional CBF by pCASL as well as for collateral flow mapping by ssASL to support delicate treatment decisions (► Fig. 5).

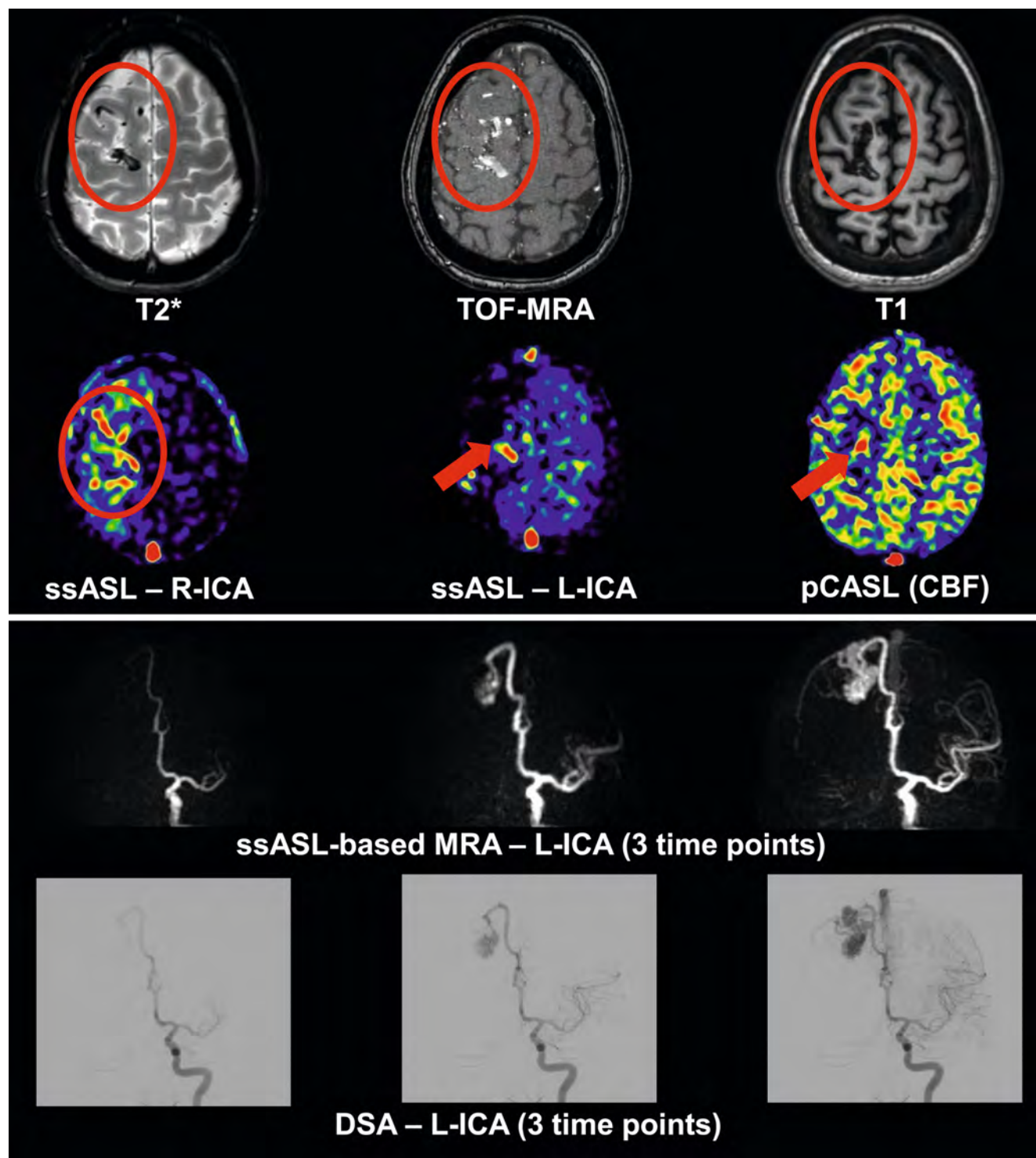
A recent study by Göttler et al. evaluated cerebral perfusion in asymptomatic patients with unilateral high-grade ICAS using pCASL [69]. Even in those asymptomatic patients, significant hypoperfusion was found [69]. Correlations of lateralized perfusion deficits with ipsilateral attention bias were shown as well [69]. Moreover, CBF was ipsilaterally decreased by around -18% compared to the contralateral hemisphere in such patients [70]. This is in good agreement with previous positron emission tomography (PET), DSC-MRI, and ASL studies [71–73]. Detailed comparisons of six hemodynamic parameters in the same study cohort by Kaczmarz et al. revealed the most severe pathophysiologic effects for CBF, as measured by pCASL [70]. While the absolute contralateral CBF values were comparable to age-matched healthy controls, their variability was increased by around $+22\%$ in ICAS [70]. This can be explained by collateral flow via the circle of Willis, which could be evaluated by ssASL.

Comparisons of pCASL, ssASL, and DSC-MRI in ICAS highlight the plausibility of ASL-based measurements and provide additional insights by mapping perfusion territory shifts. Moreover, vessel-selective ASL enables the delineation of individual border zones between perfusion territories [74, 75]. Spatial variability of those individual watershed areas (iWSAs) can be increased in patients with ICAS. Moreover, hemodynamic impairments were enhanced by up to $+117\%$ within iWSAs compared to brain regions outside of iWSAs [70]. As an alternative to vessel-selective ASL, perfusion territory border zones can be also assessed by time-encoded ASL to map ATT, based on known perfusion delays within iWSAs [76, 77]. In this regard, Di Napoli et al. showed that the presence of arterial transit artifacts on standard pCASL perfusion maps predicted the presence of symptoms in patients with ICAS and was highly correlated to a poor collateral status within the circle of Willis [78]. Thus, the technique might be regarded as a candidate to determine indications for surgical or interventional ICAS therapy. After revascularization, hemodynamic improvement was demonstrated in asymptomatic as well as in symptomatic patients using ASL [79, 80].

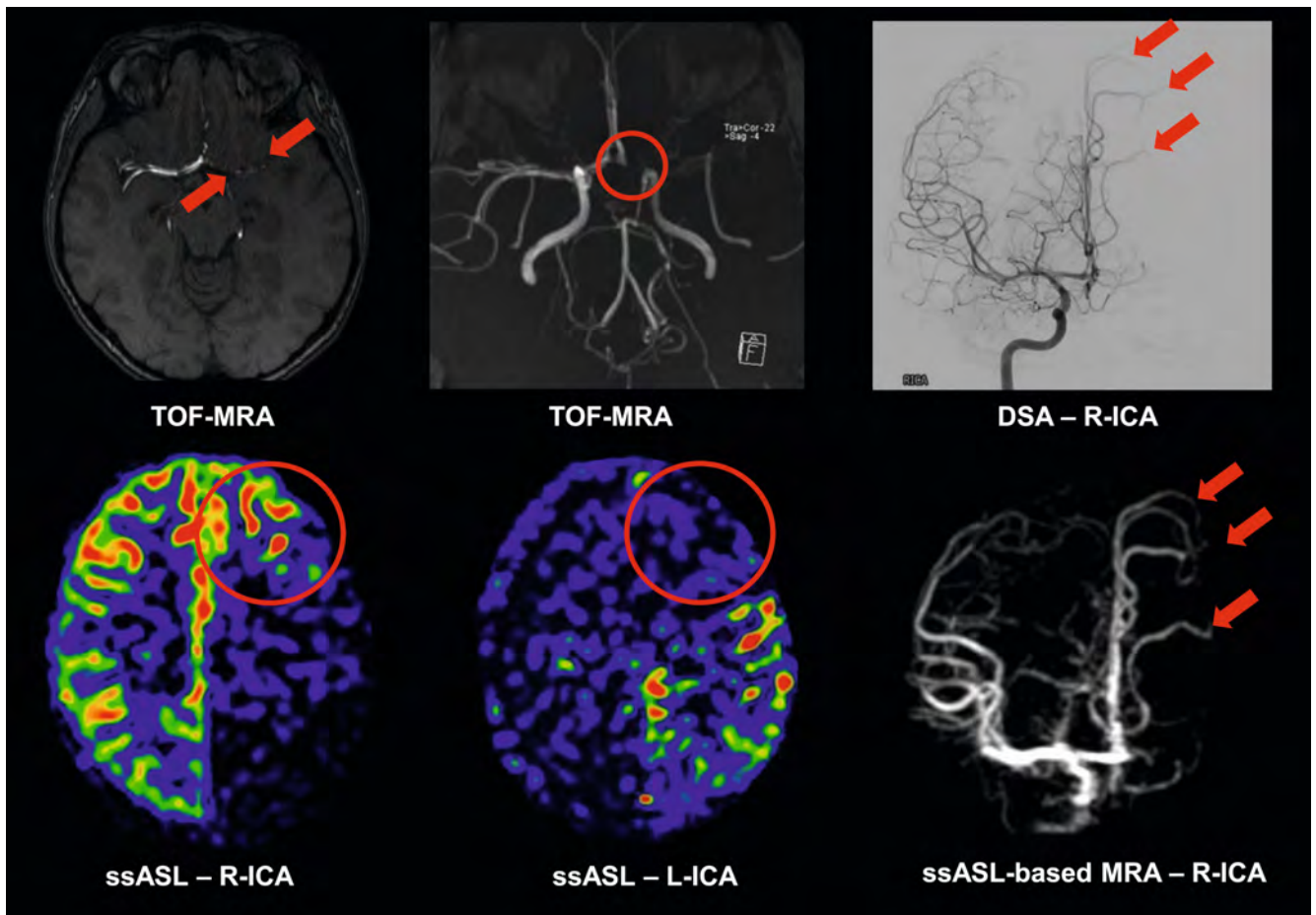
Overall, ASL may be particularly suitable for periodic application in ICAS as a noninvasive technique, including preventive screening, disease progression monitoring of patients receiving best medical treatment, or treatment efficacy testing after revascularization.

Gliomas

Gliomas are heterogeneous neuroepithelial tumors that stem from the glial cells and show an age-adjusted average rate of 6.03 per 100 000 of the population [81]. Those tumors are commonly categorized into low-grade glioma (LGG, grades 1 and 2) and high-grade glioma (HGG, grades 3 and 4) in relation to the World Health Organization (WHO) Classification of Tumors of the CNS [82]. Typically, first-line treatment includes maximum neuro-



► **Fig. 3** 50-year-old male patient with a right-hemispheric arteriovenous malformation (AVM) as indicated by irregular vessels according to susceptibility artifacts on axial T2*-weighted imaging, flow voids on axial time-of-flight magnetic resonance angiography (TOF-MRA), and hypointense tubular structures on axial non-contrast-enhanced T1-weighted imaging. According to perfusion maps from super-selective arterial spin labeling (ssASL), the AVM showed marked hyperperfusion, while parts of the right superior frontal gyrus appeared without clear perfusion for labeling of the right internal carotid artery (R-ICA). For labeling of the left ICA (L-ICA), hyperperfusion in projection on the location of the AVM can still be observed, together with perfusion of parts of the right-hemispheric superior frontal gyrus from the contralateral side. The cerebral blood flow (CBF) maps from whole-brain pseudo-continuous ASL (pCASL) resemble hyperperfusion in projection on the location of the AVM. ASL-based MRA (4D-sPACK) derived from labeling of the L-ICA showed that the right-hemispheric AVM was to large extents supplied by the left anterior cerebral artery with early venous drainage according to the third image of the time series, in agreement with the results from digital subtraction angiography (DSA) for the L-ICA.



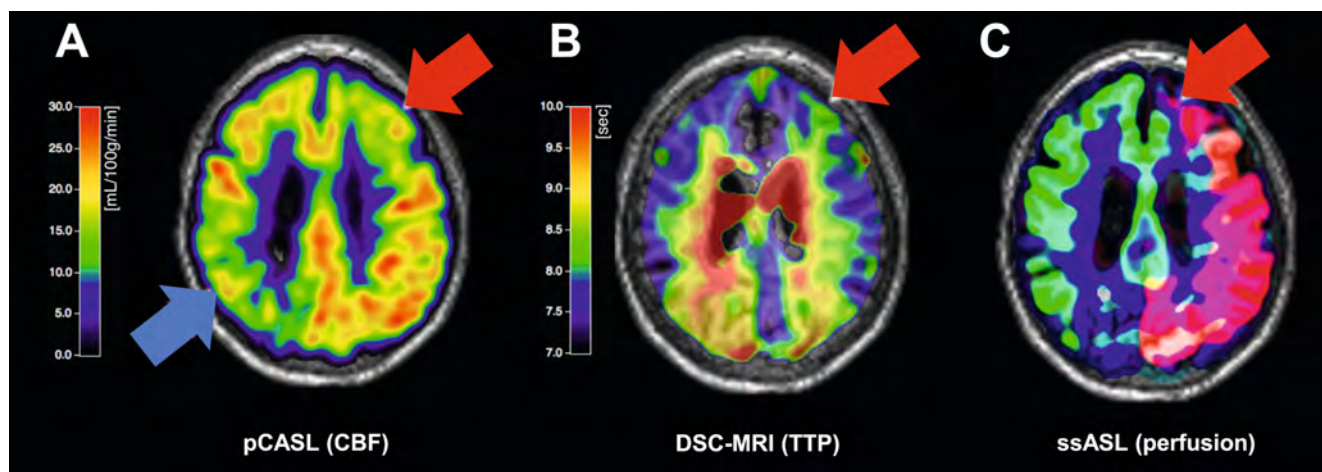
► **Fig. 4** 26-year-old female patient with Moyamoya disease showing multiple changes of arterial vessel calibers and reduced flow signals on time-of-flight magnetic resonance angiography (TOF-MRA), particularly for the left internal carotid artery (L-ICA) and left middle cerebral artery. According to perfusion maps derived from super-selective arterial spin labeling (ssASL), large areas of the left anterior frontal lobe were supplied by the right ICA (R-ICA), as indicated by increased perfusion within this location when the R-ICA was labeled and lacking perfusion when the L-ICA was labeled. Correspondingly, ASL-based MRA (4D-sPACK) with labeling of the R-ICA depicted multiple arterial branches extending to the contralateral hemisphere, which was in agreement with results from digital subtraction angiography (DSA).

surgical tumor resection for cytoreduction and to avoid complications, with the aim of prolonging survival and improving quality of life [83, 84]. In this context, ASL-based perfusion imaging can be applied for several purposes, including differential diagnosis, pre-operative tumor characterization and phenotyping, as well as monitoring of treatment response after surgery (► **Fig. 6**).

Regarding initial tumor phenotyping, differential diagnosis, and monitoring of therapy, multi-parametric advanced MRI has an emerging role [85–87]. Specifically, ASL-based perfusion imaging can delineate heightened CBF in glioma, and it has been demonstrated that it can differentiate glioma from other intracranial neoplasms such as lymphoma, metastases, or brain abscess (► **Fig. 6**) [88, 89]. It has also been shown that ASL can facilitate distinguishing between LGG and HGG, with CBF being typically significantly higher in HGG than in LGG [90]. This is due to higher perfusion and vascularity in HGG as compared to LGG, which is related to higher tumor tissue metabolism and neovascularization profiles [91, 92]. Two meta-analyses provided cumulative evidence for the role of ASL in differentiating between LGG and HGG, indicating that absolute and relative tumor blood flow val-

ues could support grading, with a pooled sensitivity of 86 %, specificity of 84 %, and an area under the curve (AUC) of 91 % for differentiating LGG from HGG [32, 93]. Besides categorization into LGG and HGG, ASL-derived tumor perfusion has been associated with multiple markers that can impact treatment decision making and survival, including isocitrate dehydrogenase status, methyl-guanine-DNA methyltransferase promoter methylation, p53 status, as well as vascular endothelial growth factor expression and tumor microvascular density [94–97]. Furthermore, it has also been suggested that malignant progression within 12 months could be predicted with ASL-based perfusion imaging in patients with LGG, with a sensitivity of 73 %, specificity of 82 %, and odds ratio of 12 [98].

Regarding monitoring of treatment response, the main purpose of perfusion imaging in glioma is to differentiate true tumor relapse or progression from treatment-induced alterations. Specifically, in HGG, pseudoprogression can typically appear as early changes within a few months after treatment (particularly after radiotherapy and/or temozolomide), while pseudoresponse can take effect after the administration of anti-angiogenic agents



► **Fig. 5** 71-year-old female patient with right-sided high-grade asymptomatic internal carotid artery stenosis (ICAS). **A** Cerebral blood flow (CBF) derived from imaging with pseudo-continuous arterial spin labeling (pCASL) showed ipsilateral decreases (blue arrow), while at the same time, contralateral frontal CBF was decreased (red arrow). **B** These findings were in agreement with delayed perfusion from dynamic susceptibility contrast magnetic resonance imaging (DSC-MRI)-based time-to-peak (TTP) assessments regarding the same location. **C** Super-selective ASL (ssASL) provided additional insight, showing that the right ICA (R-ICA) perfusion territory was shifted towards the contralateral hemisphere. Contralateral frontal perfusion impairments were located in the border zone between shifted territories of the R-ICA and left ICA (L-ICA).

(such as bevacizumab) [99–102]. In this context, it has been demonstrated that ASL-based perfusion imaging can distinguish predominant recurrent HGG from radiation necrosis with a sensitivity of more than 80%, which was comparable to findings from DSC-MRI and fluorodeoxyglucose PET (FDG-PET) [103]. Moreover, in patients with HGG who developed progressively enhancing lesions within the radiation field after resection and chemoradiation, ASL-derived CBF demonstrated the highest AUC of 0.95 and misclassified the fewest cases regarding true progression versus pseudoprogression [104].

Overall, ASL for glioma imaging has the potential of restricting administration of contrast agents, which might be relevant in light of gadolinium deposition particularly for frequent follow-up examinations as regularly scheduled in patients with glioma [105]. Furthermore, compared to DSC-MRI, ASL-based perfusion measurements should not be biased by blood-brain barrier (BBB) permeability effects, given that water is a freely diffusible tracer. In contrast, DSC-MRI relies on gadolinium-based contrast agents, which are intravascular tracers and therefore, even after leakage corrections, DSC-MRI-based perfusion estimates may be deteriorated by BBB leakage [106].

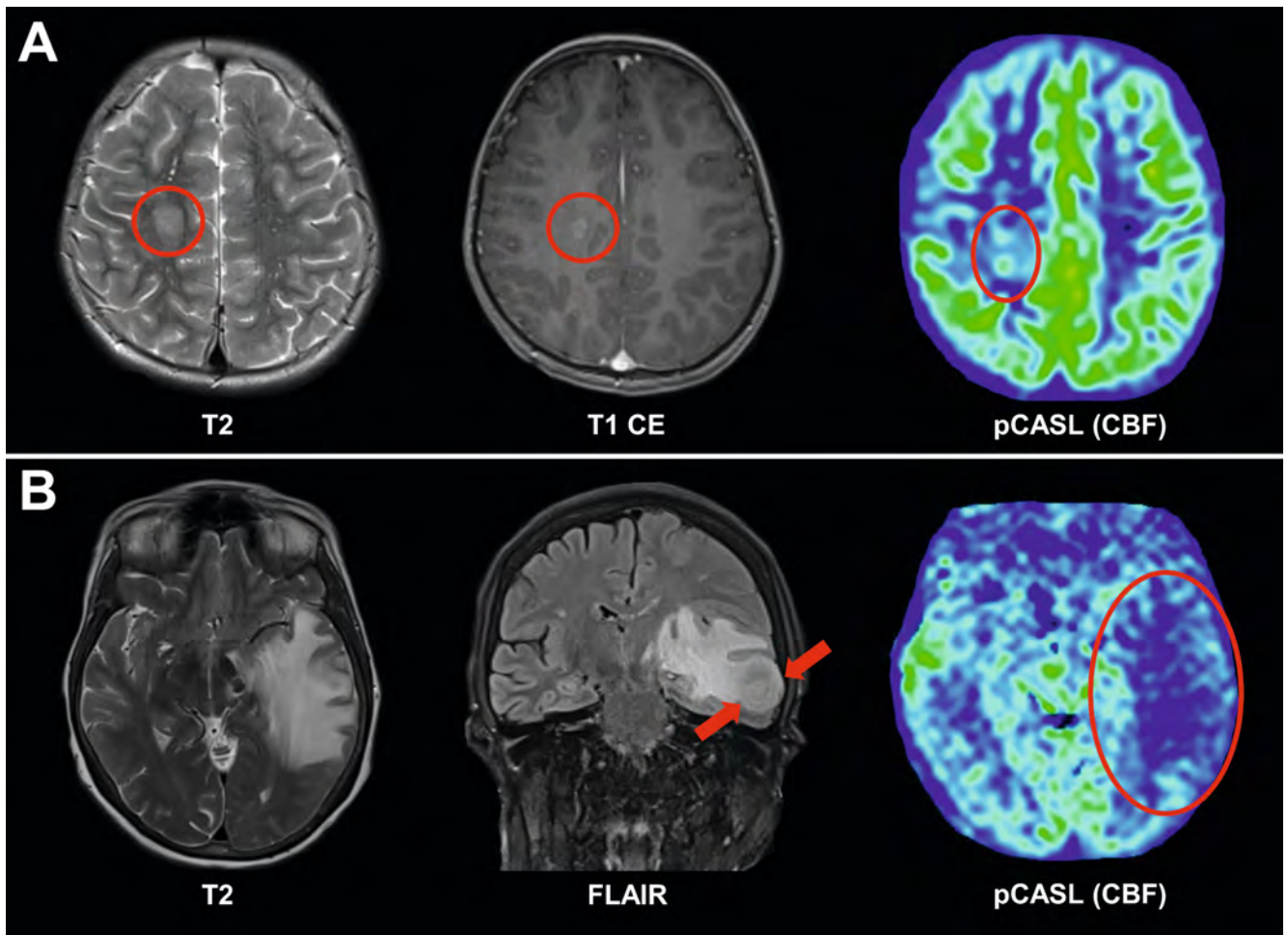
Neurodegenerative diseases

Typically characterized by a progressive loss of specific neuron populations, NDs become increasingly prevalent with aging and can be classified according to primary clinical features including Alzheimer's disease (AD), other dementia syndromes, and Parkinson's disease (PD) [107, 108]. The most common NDs are proteinopathies, which can lead to abnormal conformational properties [109]. Because of the increasing deposition of the proteins in the cerebral parenchyma, the final pathway is increasing permeability of the BBB, a decreasing expression of different receptors, and a disrupted structural and functional connectivity of nervous fibers [110].

In this context, CBF is thought to act as a proxy for synaptic activity throughout the parenchymal changes [111]. Specifically, a study comparing ASL-based perfusion and FDG-PET in patients with mild-to-moderate AD reported a considerable overlap between the hypometabolic areas from PET and the hypoperfusion areas from ASL imaging [112]. Typically, AD has been characterized by hypoperfusion/hypometabolism in the predilection sites of the posterior cingulate, precuneus, and/or posterior temporal and parietal cortices [113–116]. Thus, a certain pattern of alterations in CBF may exist for AD (► **Fig. 7**). Interestingly, several studies suggested a correlation with decreased perfusion depending on the tau and amyloid burden [117, 118]. Focusing on the alterations of perfusion patterns, ASL might prospectively play a role in screening for AD, especially with regard to the US Food and Drug Administration (FDA)-approved AD medication Lecanemab, with early detection becoming even more important in light of patient selection for a certain therapy [119].

Furthermore, hypoperfusion with hypometabolism has been revealed primarily in the frontal brain in patients with frontotemporal dementia, with overall good spatial agreement between both methods, but slightly lower sensitivity, specificity, and AUC in discriminating patients from controls for ASL-based perfusion imaging compared to PET (0.75 versus 0.87) [120, 121]. For the semantic variant of primary progressive aphasia, hypoperfusion with hypometabolism has been identified in the left anterior temporal lobe [122]. With respect to PD, the characteristic propagation of alpha-synuclein pathology can disrupt normal brain function [123].

Overall, the physiological basis of the ASL technique, with its ease of repeatability, offers a great opportunity to derive measures potentially representative of metabolic information. Thus, in the future, ND may be ideally continuously classified and monitored during the course of disease by this technique. However, the inherently low SNR of ASL compared to PET may hamper



► **Fig. 6** Perfusion imaging based on pseudo-continuous arterial spin labeling (pCASL) in the presence of space-occupying intracranial lesions. **A** In an 18-year-old male patient, a T2-hyperintense lesion with discrete contrast enhancement on axial contrast-enhanced T1-weighted imaging and corresponding mild hyperperfusion on cerebral blood flow (CBF) maps was shown in the neighborhood of the right precentral gyrus, which was histopathologically confirmed as a high-grade glioma (HGG). **B** In a 39-year-old female patient, an extensive T2-hyperintense edematous lesion was detected within the left temporal lobe, with a circumscribed oval lesion in the left lateral inferior and middle temporal gyrus. In comparison to the contralateral side, the left temporal lobe showed marked hypoperfusion according to CBF maps, and the patient was diagnosed with a brain abscess after stereotactic biopsy.

detection of early changes related to ND, but future large-scale studies are needed to further explore the role of ASL in this regard.

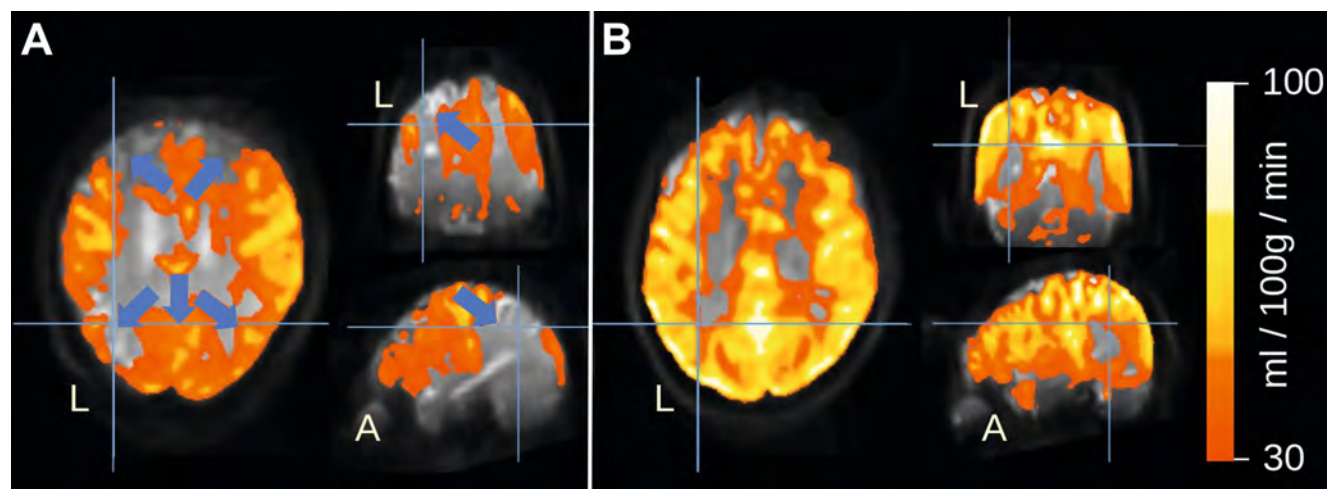
Traumatic brain injury

Worldwide, it is estimated that over 60 million incidences of traumatic brain injury (TBI) occur every year, of which approximately 80 % are considered mild TBI (mTBI) based on initial symptom presentation [124–126]. Over the last decade, ASL has emerged as a promising imaging technique for the study of cerebral perfusion changes following moderate-to-severe TBI as well as mTBI [127–140].

Studies in patients with moderate-to-severe TBI revealed decreased regional or global CBF years after the injury [137–140]. Moreover, a study reported reduced CBF in several cortical and subcortical regions to be correlated with injury severity, defined as the duration of post-traumatic amnesia [138]. Another

study focused on chronic vascular abnormalities in areas of tissue loss and in normal-appearing brain tissue [139]. Specifically, areas of encephalomalacia appeared to have both reduced perfusion and cerebrovascular reactivity (CVR), with the latter representing the vascular response after hypercapnic conditions [141]. Normal-appearing tissue, on the other hand, revealed only changes in CVR suggesting global vascular alterations post-TBI [139].

Findings from studies on mTBI are heterogeneous, with several studies reporting an increase in global or regional CBF in the acute and subacute phase after mTBI [127–132]. In contrast, another study found a regional decrease in CBF [131]. A study focusing on patients who required hospitalization found that global increase in CBF acutely after trauma was associated with a better clinical outcome, suggesting that increases in perfusion might represent a compensatory mechanism (i. e., metabolic or inflammatory response) [128]. In addition, a higher mean global and gray matter CBF was also found in the chronic phase post-injury [128]. However, months after mTBI, studies mostly reported



► **Fig. 7** Perfusion imaging based on pseudo-continuous arterial spin labeling (pCASL) in neurodegenerative diseases (ND). Comparison of perfusion analysis results from **A** a 58-year-old female patient diagnosed with Alzheimer's disease (AD; Mini-Mental State Examination score 19) and **B** a healthy 60-year-old female control in axial, coronal, and sagittal representations. The pCASL data were aligned to the anterior commissure-posterior commissure (AC-PC) line prior to analysis. Blue arrows indicate regions of reduced cerebral blood flow (CBF), including frontal and parietal areas in the patient. Images were thresholded at 30 ml/100 g/min.

decreased perfusion in various brain regions, such as the thalamus or in parts of the frontal and temporal lobes [133, 134]. It should be noted that there is limited evidence from longitudinal investigations suggesting increased CBF acutely and decreased CBF in the chronic phase [129]. Furthermore, it remains to be elucidated whether age at the time of injury or sex are associated with specific alterations in CBF. In this regard, previous studies have reported an increase in CBF or a decrease in CBF in adolescents [134, 135].

Overall, ASL is a promising technique for the evaluation of CBF following both moderate-to-severe TBI as well as mTBI. However, further research is needed to better characterize the underlying pathophysiology as well as the effects of important demographic variables (e. g., age and sex). Moreover, comprehensive study designs are needed to appreciate the association of CBF with other imaging measures, fluid biomarkers (e. g., neurofilaments), and outcome measures (e. g., neuropsychological function) to pave the way for CBF to serve as a marker for diagnosis and prognosis following TBI.

Migraine

Migraine belongs to the entity of primary headaches and has an estimated global prevalence of about 14 % [142]. Multiple factors contributing to the pathophysiology of migraine have been discussed, with the trigemino-vascular system playing a major role in migraine with and without aura [143]. In this context, central (including the hypothalamus, thalamus, brainstem, prefrontal dorsolateral cortex, M1, and S1) and peripheral mechanisms (including the trigeminal nerve and trigemino-cervical complex) may promote neurogenic inflammation: retrograde trigeminal delivery of vasoactive mediators including calcitonin gene-related peptide could trigger dilation of arteries and plasma exudation, which may perpetuate nociceptive excitation of the trigeminal nerve endings surrounding vessels [143–145]. Pain triggering and processing mechanisms of the respective brain structures

and modulation of their in-between networks are likely to alter patterns of brain perfusion. In addition, in migraine with aura, alterations in CBF can be observed in the context of acute aura symptoms with cortical spreading depression [143]. Thus, ASL-based techniques have been used in various designs to examine cerebral perfusion in migraine.

Some studies employed longitudinal designs to investigate changes in brain perfusion over the migraine cycle [146–149]. Herein, one study demonstrated decreased CBF in the right hypothalamus, retrosplenial cortex, and left visual cortex compared to healthy controls only pre-ictally, thus potentially emphasizing changing perfusion patterns over the migraine cycle [147]. Another study demonstrated cyclical perfusion changes within the right nucleus accumbens, right insular cortex, and right precentral gyrus, with perfusion increasing leading up to the attack, while a superior parietal lobule cluster demonstrated perfusion at its lowest during the attack and increasing afterwards [146]. Additionally, another study induced pharmaceutically triggered attacks in patients with migraine and aura and observed regional CBF increases in the ipsilateral dorsolateral pons (with respect to the most painful side) compared to baseline [148]. However, there are potentially conflicting results given that one study performed scans in migraine patients without aura both during spontaneous attacks and in the interictal state, revealing no difference in global or regional CBF between the two conditions [149].

Other studies employed cross-sectional designs to investigate cerebral perfusion in migraine [150–155]. Specifically, reduced CBF was described in the left nucleus accumbens of patients with interictal chronic migraine and in the cerebellar vermis of patients suffering from interictal migraine without aura [150, 151]. Furthermore, elevated CBF was found in the right V5 and superior temporal gyrus of patients with interictal migraine with aura, and in the right orbitofrontal gyrus and middle frontal gyrus, as well as for the bilateral somatosensory cortex and left primary motor cor-

tex among patients with interictal migraine without aura [150, 152–154]. Regional CBF differences between migraine patients with and without aura as well as healthy controls (in the superior frontal gyrus, postcentral gyrus, cerebellum, middle frontal gyrus, thalamus, and occipital cortex) have additionally been used to establish a support vector machine classifier, which achieved an AUC of 0.86 for differentiating migraine with and without aura [155].

Mostly due to its noninvasive nature, ASL-based perfusion imaging has also been used in cases of pediatric migraine [156–159]. A series investigating 12 pediatric cases demonstrated changes in cerebral perfusion corresponding to aura symptoms (mostly transient paresis), with a relationship between the time to symptom onset and perfusion changes [156]. Specifically, the authors observed early hypoperfusion and later hyperperfusion [156]. A similar pattern of initial hypoperfusion followed by hyperperfusion in aura-corresponding regions was observed in a case-control study of 10 pediatric patients and matched controls, albeit with differences regarding the timing of phase transition [159]. An analysis conducted in a larger cohort of 49 pediatric patients demonstrated localized hypoperfusion in all cases scanned within 24 hours of symptom onset, while patients scanned after a longer interval for the most part demonstrated normal perfusion [157]. Another study in pediatric migraine patients with a median time-to-scan interval of almost two hours after symptom onset demonstrated hypoperfusion matching neurological symptoms in 14/15 cases [158].

Overall, findings currently show little overlap between studies for adult patients, likely due to the inherent heterogeneity of migraine as a disease, as well as the rather infrequent use of ASL-based techniques in migraine to date. In pediatric migraine, however, multiple reports converge on the finding of cerebral hypoperfusion matching aura symptoms in the early phase after symptom onset. Furthermore, ASL-based perfusion imaging may also show promise with respect to investigating the specific pathological mechanisms of migraine and their association with vascular and/or global or regional perfusion alterations.

Conclusion

For many clinical use cases, perfusion imaging by ASL may be a viable alternative to conventional perfusion MRI methods that are dependent on intravenous injection of a gadolinium-based contrast agent. Since ASL works with labeling of blood-water as an endogenous tracer, caveats concerning the administration of gadolinium can be circumvented, thus making the technique particularly appealing for investigations in pediatric cohorts, patients with impaired kidney function, patients with relevant allergies, or patients who require serial imaging (e.g., due to disease monitoring for brain tumors). Beyond that, recent advances making use of vessel-selective labeling by ssASL or ASL-based MRA (4D-sPACK) can enable spatial perfusion territory mapping or time-resolved delineation of single intracranial vessels, which would not be possible using conventional contrast-based perfusion MRI methods.

Conflict of Interest

Stephan Kaczmarz is an employee of Philips GmbH, Hamburg, Germany. All other authors declare that they have no conflict of interest.

References

- [1] McGehee BE, Pollock JM, Maldjian JA. Brain perfusion imaging: How does it work and what should I use? *J Magn Reson Imaging* 2012; 36: 1257–1272. doi:10.1002/jmri.23645
- [2] Essig M, Shiroishi MS, Nguyen TB et al. Perfusion MRI: the five most frequently asked technical questions. *Am J Roentgenol* 2013; 200: 24–34. doi:10.2214/Am J Roentgenol.12.9543
- [3] Essig M, Nguyen TB, Shiroishi MS et al. Perfusion MRI: the five most frequently asked clinical questions. *Am J Roentgenol* 2013; 201: W495–W510. doi:10.2214/Am J Roentgenol.12.9544
- [4] Zaharchuk G. Theoretical basis of hemodynamic MR imaging techniques to measure cerebral blood volume, cerebral blood flow, and permeability. *AJNR Am J Neuroradiol* 2007; 28: 1850–1858. doi:10.3174/ajnr.A0831
- [5] Alsop DC, Detre JA, Golay X et al. Recommended implementation of arterial spin-labeled perfusion MRI for clinical applications: A consensus of the ISMRM perfusion study group and the European consortium for ASL in dementia. *Magn Reson Med* 2015; 73: 102–116. doi:10.1002/mrm.25197
- [6] Deibler AR, Pollock JM, Kraft RA et al. Arterial spin-labeling in routine clinical practice, part 1: technique and artifacts. *AJNR Am J Neuroradiol* 2008; 29: 1228–1234. doi:10.3174/ajnr.A1030
- [7] Deibler AR, Pollock JM, Kraft RA et al. Arterial spin-labeling in routine clinical practice, part 2: hypoperfusion patterns. *AJNR Am J Neuroradiol* 2008; 29: 1235–1241. doi:10.3174/ajnr.A1033
- [8] Deibler AR, Pollock JM, Kraft RA et al. Arterial spin-labeling in routine clinical practice, part 3: hyperperfusion patterns. *AJNR Am J Neuroradiol* 2008; 29: 1428–1435. doi:10.3174/ajnr.A1034
- [9] Hernandez-Garcia L, Aramendia-Vidaurreta V, Bolar DS et al. Recent Technical Developments in ASL: A Review of the State of the Art. *Magn Reson Med* 2022; 88: 2021–2042. doi:10.1002/mrm.29381
- [10] Detre JA, Leigh JS, Williams DS et al. Perfusion imaging. *Magn Reson Med* 1992; 23: 37–45. doi:10.1002/mrm.1910230106
- [11] Lindner T, Bolar DS, Achten E et al. Current state and guidance on arterial spin labeling perfusion MRI in clinical neuroimaging. *Magn Reson Med* 2023. doi:10.1002/mrm.29572
- [12] Kim SG. Quantification of relative cerebral blood flow change by flow-sensitive alternating inversion recovery (FAIR) technique: application to functional mapping. *Magn Reson Med* 1995; 34: 293–301. doi:10.1002/mrm.1910340303
- [13] Kwong KK, Chesler DA, Weisskoff RM et al. MR perfusion studies with T1-weighted echo planar imaging. *Magn Reson Med* 1995; 34: 878–887. doi:10.1002/mrm.1910340613
- [14] Borogovac A, Asllani I. Arterial Spin Labeling (ASL) fMRI: advantages, theoretical constraints, and experimental challenges in neurosciences. *Int J Biomed Imaging* 2012; 2012: 818456. doi:10.1155/2012/818456
- [15] Dai W, Garcia D, de Bazelaire C et al. Continuous flow-driven inversion for arterial spin labeling using pulsed radio frequency and gradient fields. *Magn Reson Med* 2008; 60: 1488–1497. doi:10.1002/mrm.21790
- [16] Garcia DM, De Bazelaire C, Alsop D. Pseudo-continuous flow driven adiabatic inversion for arterial spin labeling. In: *Proc Int Soc Magn Reson Med*. 2005 37
- [17] Buxton RB, Frank LR, Wong EC et al. A general kinetic model for quantitative perfusion imaging with arterial spin labeling. *Magn Reson Med* 1998; 40: 383–396. doi:10.1002/mrm.1910400308

- [18] Chen Y, Wang DJ, Detre JA. Comparison of arterial transit times estimated using arterial spin labeling. *MAGMA* 2012; 25: 135–144. doi:10.1007/s10334-011-0276-5
- [19] Gunther M, Bock M, Schad LR. Arterial spin labeling in combination with a look-locker sampling strategy: inflow turbo-sampling EPI-FAIR (ITS-FAIR). *Magn Reson Med* 2001; 46: 974–984. doi:10.1002/mrm.1284
- [20] van Osch MJ, Teeuwisse WM, Chen Z et al. Advances in arterial spin labelling MRI methods for measuring perfusion and collateral flow. *J Cereb Blood Flow Metab* 2018; 38: 1461–1480. doi:10.1177/0271678X17713434
- [21] Günther M. Highly efficient accelerated acquisition of perfusion inflow series by cycled arterial spin labeling. In: *Proc Intl Soc Mag Reson Med*. 2007: 380
- [22] von Samson-Himmelstjerna F, Madai VI, Sobesky J et al. Walsh-ordered hadamard time-encoded pseudocontinuous ASL (WH pCASL). *Magn Reson Med* 2016; 76: 1814–1824. doi:10.1002/mrm.26078
- [23] Hendrikse J, van der Grond J, Lu H et al. Flow territory mapping of the cerebral arteries with regional perfusion MRI. *Stroke* 2004; 35: 882–887. doi:10.1161/01.STR.0000120312.26163.EC
- [24] Golay X, Petersen ET, Hui F. Pulsed star labeling of arterial regions (PULSAR): a robust regional perfusion technique for high field imaging. *Magn Reson Med* 2005; 53: 15–21. doi:10.1002/mrm.20338
- [25] Wong EC. Vessel-encoded arterial spin-labeling using pseudocontinuous tagging. *Magn Reson Med* 2007; 58: 1086–1091. doi:10.1002/mrm.21293
- [26] Gevers S, Bokkers RP, Hendrikse J et al. Robustness and reproducibility of flow territories defined by planning-free vessel-encoded pseudocontinuous arterial spin-labeling. *AJNR Am J Neuroradiol* 2012; 33: E21–E25. doi:10.3174/ajnr.A2410
- [27] Helle M, Rufer S, van Osch MJ et al. Superselective arterial spin labeling applied for flow territory mapping in various cerebrovascular diseases. *J Magn Reson Imaging* 2013; 38: 496–503. doi:10.1002/jmri.24041
- [28] Helle M, Wenzel F, van de Ven K et al. Advanced Automatic Planning for Super-Selective Arterial Spin Labeling Flow Territory Mapping. In: *Proc Int Soc Magn Reson Med*. 2018: 302
- [29] Obara M, Togao O, Beck GM et al. Non-contrast enhanced 4D intracranial MR angiography based on pseudo-continuous arterial spin labeling with the keyhole and view-sharing technique. *Magn Reson Med* 2018; 80: 719–725. doi:10.1002/mrm.27074
- [30] Togao O, Obara M, Helle M et al. Vessel-selective 4D-MR angiography using super-selective pseudo-continuous arterial spin labeling may be a useful tool for assessing brain AVM hemodynamics. *Eur Radiol* 2020; 30: 6452–6463. doi:10.1007/s00330-020-07057-4
- [31] Chappell MA, McConnell FAK, Golay X et al. Partial volume correction in arterial spin labeling perfusion MRI: A method to disentangle anatomy from physiology or an analysis step too far? *Neuroimage* 2021; 238: 118236. doi:10.1016/j.neuroimage.2021.118236
- [32] Alsaedi A, Doniselli F, Jager HR et al. The value of arterial spin labelling in adults glioma grading: systematic review and meta-analysis. *Oncotarget* 2019; 10: 1589–1601. doi:10.18632/oncotarget.26674
- [33] Clement P, Castellaro M, Okell TW et al. ASL-BIDS, the brain imaging data structure extension for arterial spin labeling. *Sci Data* 2022; 9: 543. doi:10.1038/s41597-022-01615-9
- [34] Gorgolewski KJ, Auer T, Calhoun VD et al. The brain imaging data structure, a format for organizing and describing outputs of neuroimaging experiments. *Sci Data* 2016; 3: 160044. doi:10.1038/sdata.2016.44
- [35] Mutsaerts H, Petr J, Groot P et al. ExploreASL: An image processing pipeline for multi-center ASL perfusion MRI studies. *Neuroimage* 2020; 219: 117031. doi:10.1016/j.neuroimage.2020.117031
- [36] Adebimpe A, Bertolero M, Dolui S et al. ASLPrep: a platform for processing of arterial spin labeled MRI and quantification of regional brain perfusion. *Nat Methods* 2022; 19: 683–686. doi:10.1038/s41597-022-01458-7
- [37] Saini V, Guada L, Yavagal DR. Global Epidemiology of Stroke and Access to Acute Ischemic Stroke Interventions. *Neurology* 2021; 97: S6–S16. doi:10.1212/WNL.00000000000012781
- [38] Ornello R, Degan D, Tiseo C et al. Distribution and Temporal Trends From 1993 to 2015 of Ischemic Stroke Subtypes: A Systematic Review and Meta-Analysis. *Stroke* 2018; 49: 814–819. doi:10.1161/STROKEAHA.117.020031
- [39] Albers GW, Marks MP, Kemp S et al. Thrombectomy for Stroke at 6 to 16 Hours with Selection by Perfusion Imaging. *N Engl J Med* 2018; 378: 708–718. doi:10.1056/NEJMoa1713973
- [40] Kidwell CS, Jahan R, Gornbein J et al. A trial of imaging selection and endovascular treatment for ischemic stroke. *N Engl J Med* 2013; 368: 914–923. doi:10.1056/NEJMoa1212793
- [41] Ringleb P, Bendszus M, Bluhmki E et al. Extending the time window for intravenous thrombolysis in acute ischemic stroke using magnetic resonance imaging-based patient selection. *Int J Stroke* 2019; 14: 483–490. doi:10.1177/1747493019840938
- [42] Davis SM, Donnan GA, Parsons MW et al. Effects of alteplase beyond 3h after stroke in the Echoplanar Imaging Thrombolytic Evaluation Trial (EPITHET): a placebo-controlled randomised trial. *Lancet Neurol* 2008; 7: 299–309. doi:10.1016/S1474-4422(08)70044-9
- [43] Furlan AJ, Eyding D, Albers GW et al. Dose Escalation of Desmoteplase for Acute Ischemic Stroke (DEDAS): evidence of safety and efficacy 3 to 9 hours after stroke onset. *Stroke* 2006; 37: 1227–1231. doi:10.1161/01.STR.0000217403.66996.6d
- [44] Hacke W, Albers G, Al-Rawi Y et al. The Desmoteplase in Acute Ischemic Stroke Trial (DIAS): a phase II MRI-based 9-hour window acute stroke thrombolysis trial with intravenous desmoteplase. *Stroke* 2005; 36: 66–73. doi:10.1161/01.STR.0000149938.08731.2c
- [45] Nogueira RG, Jadhav AP, Haussen DC et al. Thrombectomy 6 to 24 Hours after Stroke with a Mismatch between Deficit and Infarct. *N Engl J Med* 2018; 378: 11–21. doi:10.1056/NEJMoa1706442
- [46] Hacke W, Furlan AJ, Al-Rawi Y et al. Intravenous desmoteplase in patients with acute ischaemic stroke selected by MRI perfusion-diffusion weighted imaging or perfusion CT (DIAS-2): a prospective, randomised, double-blind, placebo-controlled study. *Lancet Neurol* 2009; 8: 141–150. doi:10.1016/S1474-4422(08)70267-9
- [47] Ma H, Campbell BCV, Parsons MW et al. Thrombolysis Guided by Perfusion Imaging up to 9 Hours after Onset of Stroke. *N Engl J Med* 2019; 380: 1795–1803. doi:10.1056/NEJMoa1813046
- [48] Campbell BC, Mitchell PJ, Kleinig TJ et al. Endovascular therapy for ischemic stroke with perfusion-imaging selection. *N Engl J Med* 2015; 372: 1009–1018. doi:10.1056/NEJMoa1414792
- [49] Mirasol RV, Bokkers RP, Hernandez DA et al. Assessing reperfusion with whole-brain arterial spin labeling: a noninvasive alternative to gadolinium. *Stroke* 2014; 45: 456–461. doi:10.1161/STROKEAHA.113.004001
- [50] Wang DJ, Alger JR, Qiao JX et al. The value of arterial spin-labeled perfusion imaging in acute ischemic stroke: comparison with dynamic susceptibility contrast-enhanced MRI. *Stroke* 2012; 43: 1018–1024. doi:10.1161/STROKEAHA.111.631929
- [51] Bokkers RP, Hernandez DA, Merino JG et al. Whole-brain arterial spin labeling perfusion MRI in patients with acute stroke. *Stroke* 2012; 43: 1290–1294. doi:10.1161/STROKEAHA.110.589234
- [52] Bivard A, Stanwell P, Levi C et al. Arterial spin labeling identifies tissue salvage and good clinical recovery after acute ischemic stroke. *J Neuroimaging* 2013; 23: 391–396. doi:10.1111/j.1552-6569.2012.00728.x
- [53] Lu SS, Cao YZ, Su CQ et al. Hyperperfusion on Arterial Spin Labeling MRI Predicts the 90-Day Functional Outcome After Mechanical Thrombectomy in Ischemic Stroke. *J Magn Reson Imaging* 2021; 53: 1815–1822. doi:10.1002/jmri.27455

- [54] Yu S, Liebeskind DS, Dua S et al. Postischemic hyperperfusion on arterial spin labeled perfusion MRI is linked to hemorrhagic transformation in stroke. *J Cereb Blood Flow Metab* 2015; 35: 630–637. doi:10.1038/jcbfm.2014.238
- [55] Okazaki S, Yamagami H, Yoshimoto T et al. Cerebral hyperperfusion on arterial spin labeling MRI after reperfusion therapy is related to hemorrhagic transformation. *J Cereb Blood Flow Metab* 2017; 37: 3087–3090. doi:10.1177/0271678X17718099
- [56] Raman A, Upreti M, Calero MJ et al. A Systematic Review Comparing Digital Subtraction Angiogram With Magnetic Resonance Angiogram Studies in Demonstrating the Angioarchitecture of Cerebral Arteriovenous Malformations. *Cureus* 2022; 14: e25803. doi:10.7759/cureus.25803
- [57] Hernandez Petzsche MR, Reichert M, Hoffmann G et al. Non-invasive perfusion territory quantification and time-resolved angiography by arterial spin labeling in a patient with a large right-hemispheric AVM: case report. *J Neurol* 2022; 269: 4539–4545. doi:10.1007/s00415-022-11065-3
- [58] Heit JJ, Thakur NH, Iv M et al. Arterial-spin labeling MRI identifies residual cerebral arteriovenous malformation following stereotactic radiosurgery treatment. *J Neuroradiol* 2020; 47: 13–19. doi:10.1016/j.neurad.2018.12.004
- [59] Rojas-Villabona A, Pizzini FB, Solbach T et al. Are Dynamic Arterial Spin-Labeling MRA and Time-Resolved Contrast-Enhanced MRA Suited for Confirmation of Obliteration following Gamma Knife Radiosurgery of Brain Arteriovenous Malformations? *AJNR Am J Neuroradiol* 2021; 42: 671–678. doi:10.3174/ajnr.A6990
- [60] Sollmann N, Liebl H, Preibisch C et al. Super-selective ASL and 4D ASL-based MR Angiography in a Patient with Moyamoya Disease: Case Report. *Clin Neuroradiol* 2021; 31: 515–519. doi:10.1007/s00062-020-00961-8
- [61] Yu Z, Bai X, Zhang Y et al. Baseline Hemodynamic Impairment and Revascularization Outcome in Newly Diagnosed Adult Moyamoya Disease Determined by Pseudocontinuous Arterial Spin Labeling. *World Neurosurg* 2022; 165: e494–e504. doi:10.1016/j.wneu.2022.06.084
- [62] Flaherty ML, Kissela B, Khoury JC et al. Carotid artery stenosis as a cause of stroke. *Neuroepidemiology* 2013; 40: 36–41. doi:10.1159/000341410
- [63] Petty GW, Brown RD Jr., Whisnant JP et al. Ischemic stroke subtypes: a population-based study of incidence and risk factors. *Stroke* 1999; 30: 2513–2516. doi:10.1161/01.str.30.12.2513
- [64] Uchino K, Risser JM, Smith MA et al. Ischemic stroke subtypes among Mexican Americans and non-Hispanic whites: the BASIC Project. *Neurology* 2004; 63: 574–576. doi:10.1212/01.wnl.0000133212.99040.07
- [65] Marshall RS, Lazar RM, Liebeskind DS et al. Carotid revascularization and medical management for asymptomatic carotid stenosis – Hemodynamics (CREST-H): Study design and rationale. *Int J Stroke* 2018; 13: 985–991. doi:10.1177/1747493018790088
- [66] Grant EG, Benson CB, Moneta GL et al. Carotid artery stenosis: gray-scale and Doppler US diagnosis—Society of Radiologists in Ultrasound Consensus Conference. *Radiology* 2003; 229: 340–346. doi:10.1148/radiol.2292030516
- [67] von Reutern GM, Goertler MW, Bornstein NM et al. Grading carotid stenosis using ultrasonic methods. *Stroke* 2012; 43: 916–921. doi:10.1161/STROKEAHA.111.636084
- [68] Liebeskind DS, Cotsonis GA, Saver JL et al. Collaterals dramatically alter stroke risk in intracranial atherosclerosis. *Ann Neurol* 2011; 69: 963–974. doi:10.1002/ana.22354
- [69] Gottler J, Kaczmarz S, Nuttall R et al. The stronger one-sided relative hypoperfusion, the more pronounced ipsilateral spatial attentional bias in patients with asymptomatic carotid stenosis. *J Cereb Blood Flow Metab* 2020; 40: 314–327. doi:10.1177/0271678X18815790
- [70] Kaczmarz S, Gottler J, Petr J et al. Hemodynamic impairments within individual watershed areas in asymptomatic carotid artery stenosis by multimodal MRI. *J Cereb Blood Flow Metab* 2021; 41: 380–396. doi:10.1177/0271678X20912364
- [71] Lythgoe DJ, Ostergaard L, William SC et al. Quantitative perfusion imaging in carotid artery stenosis using dynamic susceptibility contrast-enhanced magnetic resonance imaging. *Magn Reson Imaging* 2000; 18: 1–11. doi:10.1016/s0730-725x(99)00112-5
- [72] Bouvier J, Detante O, Tahon F et al. Reduced CMRO(2) and cerebrovascular reserve in patients with severe intracranial arterial stenosis: a combined multiparametric qBOLD oxygenation and BOLD fMRI study. *Hum Brain Mapp* 2015; 36: 695–706. doi:10.1002/hbm.22657
- [73] Gibbs JM, Wise RJ, Leenders KL et al. Evaluation of cerebral perfusion reserve in patients with carotid-artery occlusion. *Lancet* 1984; 1: 310–314. doi:10.1016/s0140-6736(84)90361-1
- [74] Hartkamp NS, Petersen ET, Chappell MA et al. Relationship between haemodynamic impairment and collateral blood flow in carotid artery disease. *J Cereb Blood Flow Metab* 2018; 38: 2021–2032. doi:10.1177/0271678X17724027
- [75] van Laar PJ, Hendrikse J, Klijn CJ et al. Symptomatic carotid artery occlusion: flow territories of major brain-feeding arteries. *Radiology* 2007; 242: 526–534. doi:10.1148/radiol.2422060179
- [76] Petersen ET, Mouridsen K, Golay X et al. The QUASAR reproducibility study, Part II: Results from a multi-center Arterial Spin Labeling test-retest study. *Neuroimage* 2010; 49: 104–113. doi:10.1016/j.neuroimage.2009.07.068
- [77] Hendrikse J, Petersen ET, van Laar PJ et al. Cerebral border zones between distal end branches of intracranial arteries: MR imaging. *Radiology* 2008; 246: 572–580. doi:10.1148/radiol.2461062100
- [78] Di Napoli A, Cheng SF, Gregson J et al. Arterial Spin Labeling MRI in Carotid Stenosis: Arterial Transit Artifacts May Predict Symptoms. *Radiology* 2020; 297: 652–660. doi:10.1148/radiol.2020200225
- [79] Schroder J, Heinze M, Gunther M et al. Dynamics of brain perfusion and cognitive performance in revascularization of carotid artery stenosis. *Neuroimage Clin* 2019; 22: 101779. doi:10.1016/j.nicl.2019.101779
- [80] Yun TJ, Sohn CH, Han MH et al. Effect of carotid artery stenting on cerebral blood flow: evaluation of hemodynamic changes using arterial spin labeling. *Neuroradiology* 2013; 55: 271–281. doi:10.1007/s00234-012-1104-y
- [81] Miller KD, Ostrom QT, Kruchko C et al. Brain and other central nervous system tumor statistics, 2021. *CA Cancer J Clin* 2021; 71: 381–406. doi:10.3322/caac.21693
- [82] Louis DN, Perry A, Wesseling P et al. The 2021 WHO Classification of Tumors of the Central Nervous System: a summary. *Neuro Oncol* 2021; 23: 1231–1251. doi:10.1093/neuonc/noab106
- [83] Stupp R, Brada M, van den Bent MJ et al. High-grade glioma: ESMO Clinical Practice Guidelines for diagnosis, treatment and follow-up. *Ann Oncol* 2014; 25 (Suppl. 3): iii93–iii101. doi:10.1093/annonc/mdl050
- [84] Sim HW, Morgan ER, Mason WP. Contemporary management of high-grade gliomas. *CNS Oncol* 2018; 7: 51–65. doi:10.2217/cns-2017-0026
- [85] Kassubeck R, Muller HP, Thiele A et al. Advanced magnetic resonance imaging to support clinical drug development for malignant glioma. *Drug Discov Today* 2021; 26: 429–441. doi:10.1016/j.drudis.2020.11.023
- [86] van Santwijk L, Kouwenberg V, Meijer F et al. A systematic review and meta-analysis on the differentiation of glioma grade and mutational status by use of perfusion-based magnetic resonance imaging. *Insights Imaging* 2022; 13: 102. doi:10.1186/s13244-022-01230-7
- [87] Smits M. Update on neuroimaging in brain tumours. *Curr Opin Neurol* 2021; 34: 497–504. doi:10.1097/WCO.0000000000000950
- [88] You SH, Yun TJ, Choi HJ et al. Differentiation between primary CNS lymphoma and glioblastoma: qualitative and quantitative analysis using arterial spin labeling MR imaging. *Eur Radiol* 2018; 28: 3801–3810. doi:10.1007/s00330-018-5359-5

- [89] Lin L, Xue Y, Duan Q et al. The role of cerebral blood flow gradient in peritumoral edema for differentiation of glioblastomas from solitary metastatic lesions. *Oncotarget* 2016; 7: 69051–69059. doi:10.18632/oncotarget.12053
- [90] Zeng Q, Jiang B, Shi F et al. 3D Pseudocontinuous Arterial Spin-Labeling MR Imaging in the Preoperative Evaluation of Gliomas. *AJNR Am J Neuroradiol* 2017; 38: 1876–1883. doi:10.3174/ajnr.A5299
- [91] Yuan F, Salehi HA, Boucher Y et al. Vascular permeability and microcirculation of gliomas and mammary carcinomas transplanted in rat and mouse cranial windows. *Cancer Res* 1994; 54: 4564–4568
- [92] Roberts HC, Roberts TP, Brasch RC et al. Quantitative measurement of microvascular permeability in human brain tumors achieved using dynamic contrast-enhanced MR imaging: correlation with histologic grade. *AJNR Am J Neuroradiol* 2000; 21: 891–899
- [93] Kong L, Chen H, Yang Y et al. A meta-analysis of arterial spin labelling perfusion values for the prediction of glioma grade. *Clin Radiol* 2017; 72: 255–261. doi:10.1016/j.crad.2016.10.016
- [94] Mao J, Deng D, Yang Z et al. Pretreatment structural and arterial spin labeling MRI is predictive for p53 mutation in high-grade gliomas. *Br J Radiol* 2020; 93: 20200661. doi:10.1259/bjr.20200661
- [95] Yoo RE, Yun TJ, Hwang I et al. Arterial spin labeling perfusion-weighted imaging aids in prediction of molecular biomarkers and survival in glioblastomas. *Eur Radiol* 2020; 30: 1202–1211. doi:10.1007/s00330-019-06379-2
- [96] Dangouloff-Ros V, Deroulers C, Foissac F et al. Arterial Spin Labeling to Predict Brain Tumor Grading in Children: Correlations between Histopathologic Vascular Density and Perfusion MR Imaging. *Radiology* 2016; 281: 553–566. doi:10.1148/radiol.2016152228
- [97] Pang H, Dang X, Ren Y et al. 3D-ASL perfusion correlates with VEGF expression and overall survival in glioma patients: Comparison of quantitative perfusion and pathology on accurate spatial location-matched basis. *J Magn Reson Imaging* 2019; 50: 209–220. doi:10.1002/jmri.26562
- [98] Flies CM, Snijders TJ, Van Seeters T et al. Perfusion imaging with arterial spin labeling (ASL)-MRI predicts malignant progression in low-grade (WHO grade II) gliomas. *Neuroradiology* 2021; 63: 2023–2033. doi:10.1007/s00234-021-02737-4
- [99] de Wit MC, de Bruin HG, Eijkenboom W et al. Immediate post-radiotherapy changes in malignant glioma can mimic tumor progression. *Neurology* 2004; 63: 535–537. doi:10.1212/01.wnl.0000133398.11870.9a
- [100] Taal W, Brandsma D, de Bruin HG et al. Incidence of early pseudo-progression in a cohort of malignant glioma patients treated with chemoradiation with temozolomide. *Cancer* 2008; 113: 405–410. doi:10.1002/cncr.23562
- [101] Hygino da Cruz LC Jr., Rodriguez I, Domingues RC et al. Pseudoprogression and pseudoresponse: imaging challenges in the assessment of posttreatment glioma. *AJNR Am J Neuroradiol* 2011; 32: 1978–1985. doi:10.3174/ajnr.A2397
- [102] Jeck J, Kassubek R, Coburger J et al. Bevacizumab in temozolomide refractory high-grade gliomas: single-centre experience and review of the literature. *Ther Adv Neurol Disord* 2018; 11: 1756285617753597. doi:10.1177/1756285617753597
- [103] Ozsunar Y, Mullins ME, Kwong K et al. Glioma recurrence versus radiation necrosis? A pilot comparison of arterial spin-labeled, dynamic susceptibility contrast enhanced MRI, and FDG-PET imaging. *Acad Radiol* 2010; 17: 282–290. doi:10.1016/j.acra.2009.10.024
- [104] Manning P, Daghighi S, Rajaratnam MK et al. Differentiation of progressive disease from pseudoprogression using 3D PCASL and DSC perfusion MRI in patients with glioblastoma. *J Neurooncol* 2020; 147: 681–690. doi:10.1007/s11060-020-03475-y
- [105] McDonald RJ, McDonald JS, Kallmes DF et al. Intracranial Gadolinium Deposition after Contrast-enhanced MR Imaging. *Radiology* 2015; 275: 772–782. doi:10.1148/radiol.15150025
- [106] Lavrova A, Teunissen WHT, Warnert EAH et al. Diagnostic Accuracy of Arterial Spin Labeling in Comparison With Dynamic Susceptibility Contrast-Enhanced Perfusion for Brain Tumor Surveillance at 3T MRI. *Front Oncol* 2022; 12: 849657. doi:10.3389/fonc.2022.849657
- [107] Dugger BN, Dickson DW. Pathology of Neurodegenerative Diseases. *Cold Spring Harb Perspect Biol* 2017; 9. doi:10.1101/cshperspect.a028035
- [108] Hou Y, Dan X, Babbar M et al. Ageing as a risk factor for neurodegenerative disease. *Nat Rev Neurol* 2019; 15: 565–581. doi:10.1038/s41582-019-0244-7
- [109] Jucker M, Walker LC. Self-propagation of pathogenic protein aggregates in neurodegenerative diseases. *Nature* 2013; 501: 45–51. doi:10.1038/nature12481
- [110] Sweeney MD, Zhao Z, Montagne A et al. Blood-Brain Barrier: From Physiology to Disease and Back. *Physiol Rev* 2019; 99: 21–78. doi:10.1152/physrev.00050.2017
- [111] Kisler K, Nelson AR, Montagne A et al. Cerebral blood flow regulation and neurovascular dysfunction in Alzheimer disease. *Nat Rev Neurosci* 2017; 18: 419–434. doi:10.1038/nrn.2017.48
- [112] Yan L, Liu CY, Wong KP et al. Regional association of pCASL-MRI with FDG-PET and PiB-PET in people at risk for autosomal dominant Alzheimer's disease. *Neuroimage Clin* 2018; 17: 751–760. doi:10.1016/j.nicl.2017.12.003
- [113] Dolui S, Li Z, Nasrallah IM et al. Arterial spin labeling versus (18)F-FDG-PET to identify mild cognitive impairment. *Neuroimage Clin* 2020; 25: 102146. doi:10.1016/j.nicl.2019.102146
- [114] Musiek ES, Chen Y, Korczykowski M et al. Direct comparison of fluoro-deoxyglucose positron emission tomography and arterial spin labeling magnetic resonance imaging in Alzheimer's disease. *Alzheimers Dement* 2012; 8: 51–59. doi:10.1016/j.jalz.2011.06.003
- [115] Dolui S, Vidorreta M, Wang Z et al. Comparison of PASL, PCASL, and background-suppressed 3D PCASL in mild cognitive impairment. *Hum Brain Mapp* 2017; 38: 5260–5273. doi:10.1002/hbm.23732
- [116] Riederer I, Bohn KP, Preibisch C et al. Alzheimer Disease and Mild Cognitive Impairment: Integrated Pulsed Arterial Spin-Labeling MRI and (18)F-FDG PET. *Radiology* 2018; 288: 198–206. doi:10.1148/radiol.2018170575
- [117] Bryant AG, Manhard MK, Salat DH et al. Heterogeneity of Tau Deposition and Microvascular Involvement in MCI and AD. *Curr Alzheimer Res* 2021; 18: 711–720. doi:10.2174/1567205018666211126113904
- [118] Fazlollahi A, Calamante F, Liang X et al. Increased cerebral blood flow with increased amyloid burden in the preclinical phase of Alzheimer's disease. *J Magn Reson Imaging* 2020; 51: 505–513. doi:10.1002/jmri.26810
- [119] van Dyck CH, Swanson CJ, Aisen P et al. Lecanemab in Early Alzheimer's Disease. *N Engl J Med* 2023; 388: 9–21. doi:10.1056/NEJMoa2212948
- [120] Ssali T, Narciso L, Hicks J et al. Concordance of regional hypoperfusion by pCASL MRI and (15)O-water PET in frontotemporal dementia: Is pCASL an efficacious alternative? *Neuroimage Clin* 2022; 33: 102950. doi:10.1016/j.nicl.2022.102950
- [121] Anazodo UC, Finger E, Kwan BYM et al. Using simultaneous PET/MRI to compare the accuracy of diagnosing frontotemporal dementia by arterial spin labelling MRI and FDG-PET. *Neuroimage Clin* 2018; 17: 405–414. doi:10.1016/j.nicl.2017.10.033
- [122] Taswell C, Villemagne VL, Yates P et al. 18F-FDG PET Improves Diagnosis in Patients with Focal-Onset Dementias. *J Nucl Med* 2015; 56: 1547–1553. doi:10.2967/jnumed.115.161067
- [123] Poewe W, Seppi K, Tanner CM et al. Parkinson disease. *Nat Rev Dis Primers* 2017; 3: 17013. doi:10.1038/nrdp.2017.13

- [124] Dewan MC, Rattani A, Gupta S et al. Estimating the global incidence of traumatic brain injury. *J Neurosurg* 2018; 1–18. doi:10.3171/2017.10.JNS17352
- [125] Management of Concussion/m TBIWG. VA/DoD Clinical Practice Guideline for Management of Concussion/Mild Traumatic Brain Injury. *J Rehabil Res Dev* 2009; 46: CP1–CP68
- [126] Cassidy JD, Carroll LJ, Peloso PM et al. Incidence, risk factors and prevention of mild traumatic brain injury: results of the WHO Collaborating Centre Task Force on Mild Traumatic Brain Injury. *J Rehabil Med* 2004; 28–60. doi:10.1080/16501960410023732
- [127] Bai G, Bai L, Cao J et al. Sex differences in cerebral perfusion changes after mild traumatic brain injury: Longitudinal investigation and correlation with outcome. *Brain Res* 2019; 1708: 93–99. doi:10.1016/j.brainres.2018.12.018
- [128] Xu L, Ware JB, Kim JJ et al. Arterial Spin Labeling Reveals Elevated Cerebral Blood Flow with Distinct Clusters of Hypo- and Hyperperfusion after Traumatic Brain Injury. *J Neurotrauma* 2021; 38: 2538–2548. doi:10.1089/neu.2020.7553
- [129] Churchill NW, Hutchison MG, Graham SJ et al. Mapping brain recovery after concussion: From acute injury to 1 year after medical clearance. *Neurology* 2019; 93: e1980–e1992. doi:10.1212/WNL.00000000000008523
- [130] Barlow KM, Marcil LD, Dewey D et al. Cerebral Perfusion Changes in Post-Concussion Syndrome: A Prospective Controlled Cohort Study. *J Neurotrauma* 2017; 34: 996–1004. doi:10.1089/neu.2016.4634
- [131] Li F, Lu L, Shang S et al. Cerebral Blood Flow and Its Connectivity Deficits in Mild Traumatic Brain Injury at the Acute Stage. *Neural Plast* 2020; 2020: 2174371. doi:10.1155/2020/2174371
- [132] Churchill NW, Hutchison MG, Richards D et al. The first week after concussion: Blood flow, brain function and white matter microstructure. *Neuroimage Clin* 2017; 14: 480–489. doi:10.1016/j.nicl.2017.02.015
- [133] Grossman EJ, Jensen JH, Babb JS et al. Cognitive impairment in mild traumatic brain injury: a longitudinal diffusional kurtosis and perfusion imaging study. *AJNR Am J Neuroradiol* 2013; 34: 951–957. doi:10.3174/ajnr.A3358
- [134] Brooks BL, Low TA, Plourde V et al. Cerebral blood flow in children and adolescents several years after concussion. *Brain Inj* 2019; 33: 233–241. doi:10.1080/02699052.2018.1540798
- [135] Stephens JA, Liu P, Lu H et al. Cerebral Blood Flow after Mild Traumatic Brain Injury: Associations between Symptoms and Post-Injury Perfusion. *J Neurotrauma* 2018; 35: 241–248. doi:10.1089/neu.2017.5237
- [136] Zhao P, Zhu P, Zhang D et al. Sex Differences in Cerebral Blood Flow and Serum Inflammatory Cytokines and Their Relationships in Mild Traumatic Brain Injury. *Front Neurol* 2021; 12: 755152. doi:10.3389/fneur.2021.755152
- [137] Vedung F, Fahlstrom M, Wall A et al. Chronic cerebral blood flow alterations in traumatic brain injury and sports-related concussions. *Brain Inj* 2022; 36: 948–960. doi:10.1080/02699052.2022.2109746
- [138] Ware JB, Dolui S, Duda J et al. Relationship of Cerebral Blood Flow to Cognitive Function and Recovery in Early Chronic Traumatic Brain Injury. *J Neurotrauma* 2020; 37: 2180–2187. doi:10.1089/neu.2020.7031
- [139] Haber M, Amyot F, Kenney K et al. Vascular Abnormalities within Normal Appearing Tissue in Chronic Traumatic Brain Injury. *J Neurotrauma* 2018; 35: 2250–2258. doi:10.1089/neu.2018.5684
- [140] Kim J, Whyte J, Patel S et al. Resting cerebral blood flow alterations in chronic traumatic brain injury: an arterial spin labeling perfusion fMRI study. *J Neurotrauma* 2010; 27: 1399–1411. doi:10.1089/neu.2009.1215
- [141] Champagne AA, Coverdale NS, Germuska M et al. Multi-parametric analysis reveals metabolic and vascular effects driving differences in BOLD-based cerebrovascular reactivity associated with a history of sport concussion. *Brain Inj* 2019; 33: 1479–1489. doi:10.1080/02699052.2019.1644375
- [142] Stovner LJ, Hagen K, Linde M et al. The global prevalence of headache: an update, with analysis of the influences of methodological factors on prevalence estimates. *J Headache Pain* 2022; 23: 34. doi:10.1186/s10194-022-01402-2
- [143] Ashina M, Hansen JM, Do TP et al. Migraine and the trigeminovascular system—40 years and counting. *Lancet Neurol* 2019; 18: 795–804. doi:10.1016/S1474-4422(19)30185-1
- [144] Charles A. The pathophysiology of migraine: implications for clinical management. *Lancet Neurol* 2018; 17: 174–182. doi:10.1016/S1474-4422(17)30435-0
- [145] Goadsby PJ, Holland PR. An Update: Pathophysiology of Migraine. *Neurol Clin* 2019; 37: 651–671. doi:10.1016/j.ncl.2019.07.008
- [146] Stankewitz A, Keidel L, Rehm M et al. Migraine attacks as a result of hypothalamic loss of control. *Neuroimage: Clinical* 2021; 32: 102784
- [147] Meylakh N, Marciszewski KK, Di Pietro F et al. Altered regional cerebral blood flow and hypothalamic connectivity immediately prior to a migraine headache. *Cephalalgia* 2020; 40: 448–460
- [148] Younis S, Christensen CE, Vestergaard MB et al. Glutamate levels and perfusion in pons during migraine attacks: a 3T MRI study using proton spectroscopy and arterial spin labeling. *Journal of Cerebral Blood Flow & Metabolism* 2021; 41: 604–616
- [149] Gil-Gouveia R, Pinto J, Figueiredo P et al. An arterial spin labeling MRI perfusion study of migraine without aura attacks. *Frontiers in neurology* 2017; 8: 280
- [150] Zhang D, Huang X, Mao C et al. Assessment of normalized cerebral blood flow and its connectivity with migraines without aura during interictal periods by arterial spin labeling. *The Journal of Headache and Pain* 2021; 22: 1–10
- [151] Liu M, Sun Y, Li X et al. Hypoperfusion in nucleus accumbens in chronic migraine using 3D pseudo-continuous arterial spin labeling imaging MRI. *The Journal of Headache and Pain* 2022; 23: 1–7
- [152] Michels L, Villanueva J, O’Gorman R et al. Interictal hyperperfusion in the higher visual cortex in patients with episodic migraine. *Headache: The Journal of Head and Face Pain* 2019; 59: 1808–1820
- [153] Hodkinson DJ, Veggeberg R, Wilcox SL et al. Primary somatosensory cortices contain altered patterns of regional cerebral blood flow in the interictal phase of migraine. *PLoS One* 2015; 10: e0137971
- [154] Youssef AM, Ludwick A, Wilcox SL et al. In child and adult migraineurs the somatosensory cortex stands out... again: An arterial spin labeling investigation. *Human brain mapping* 2017; 38: 4078–4087
- [155] Fu T, Liu L, Huang X et al. Cerebral blood flow alterations in migraine patients with and without aura: An arterial spin labeling study. *The Journal of Headache and Pain* 2022; 23: 1–9
- [156] Cobb-Pitstick K, Munjal N, Safier R et al. Time course of cerebral perfusion changes in children with migraine with aura mimicking stroke. *American Journal of Neuroradiology* 2018; 39: 1751–1755
- [157] Uetani H, Kitajima M, Sugahara T et al. Perfusion abnormality on three-dimensional arterial spin labeling with a 3T MR system in pediatric and adolescent patients with migraine. *Journal of the Neurological Sciences* 2018; 395: 41–46
- [158] Cadiot D, Longuet R, Bruneau B et al. Magnetic resonance imaging in children presenting migraine with aura: association of hypoperfusion detected by arterial spin labelling and vasospasm on MR angiography findings. *Cephalalgia* 2018; 38: 949–958
- [159] Boulouis G, Shotar E, Dangouloff-Ros V et al. Magnetic resonance imaging arterial-spin-labelling perfusion alterations in childhood migraine with atypical aura: a case-control study. *Developmental Medicine & Child Neurology* 2016; 58: 965–969